VOLUME 14 ISSUE 4

LIDAR MAGAZINE

NOV/DEC 2024

SPECIAL ISSUE

MAPPING CARBON

AIRBORNE SHOWCASE

FRONTIER PRECISION

How You Measure Matters

PERFECTLY POSITIONED **TO GROW YOUR BUSINESS.**

NO MATTER THE SIZE OF YOUR PROJECTS, FRONTIER PRECISION HAS BEEN PROVIDING THE RIGHT SOLUTIONS SINCE 1988.

SINCE 1988

WE MAKE YOU MORE PRODUCTIVE WITH:

GEOSPATIAL

LEVERAGE YOUR DATA FOR INTELLIGENT DECISION MAKING

UNMANNED

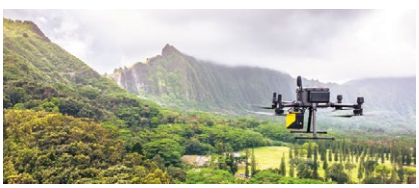

EVERY PLACE IS WITHIN REACH

BUILDING CONSTRUCTION

YOUR BLUEPRINT FOR SMART CONSTRUCTION

UNDERGROUND UTILITIES

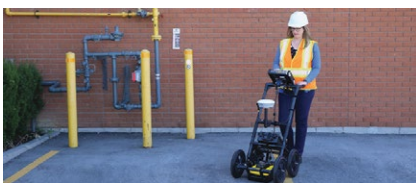

UNDERGROUND AND ABOVE GROUND SAFETY

AGRICULTURE

LEAN INTO FIELD INTELLIGENCE

SOFTWARE & PROFESSIONAL SERVICES

EDUCATION, TRAINING, AND SERVICE

CIVIL CONSTRUCTION

BETTER DECISIONS, HIGHER EFFICIENCIES

WATER RESOURCES

GO WITH THE FLOW

LEARN HOW WITH EVERY MEASUREMENT YOU TAKE, THE VALUE OF OUR EXPERTISE BECOMES IMMEASURABLE. VISIT **FRONTIERPRECISION.COM**

FRONTIER PRECISION, CORPORATE | BISMARCK 1713 BURLINGTON DRIVE, BISMARCK, ND 58504 OFFICE 701.222.2030 | TOLL FREE 800.359.3703

LIDAR MAGAZINE

IN THIS ISSUE

COLUMNS

LIDAR To Go!

Get the most from this magazine on your tablet or laptop.

◀ ON THE COVER

Digital Terrain Model (DTM) of the Anna Lotta Biosphere Reserve, located in the seasonally tropical dry forests of the Tumbesian endemic zone on the Pacific coast of Ecuador. High-resolution lidar was employed to develop this DTM, forming the foundation for ongoing monitoring and conservation strategies. The model plays a vital role in carbon sequestration and biodiversity conservation. Image courtesy LiDAR Latinoamerica, LLC

DR. A. STEWART WALKER

Lidar is everywhere!

We've packed this edition, our annual Airborne Technology Showcase, with five feature articles that illustrate lidar's growing capabilities—perhaps more importantly, how it has become the tool of choice to address a cornucopia of projects all over the world.

We lead with a piece by Nelson Mattie and Alfonso Gomez on the use of lidar to mitigate the threats to Ecuador's dry tropical forests. The sensor was a RIEGL LMS-Q680i and the software was from rapidlasso (LAStools) and BayesMap Solutions. The results were biomass and carbon stock estimations, so critical now as we finally address the results of climate change. There's a valuable section of the article where the authors summarize the advantages of full-waveform data capture and analysis.

On page 16, we have a submission from Contributing Writer Al Karlin and George Cole, centered on a fascinating bathymetric lidar project. Eight miles off the coast of Florida lies the Ochlockonee Shoal, ever since the Spanish sailed through the area in the 1630s to supply a mission. The Coast & Geodetic Survey conducted a hydrographic survey in 1881 and that appeared to be the most up-to-date until NV5 and Dewberry flew bathymetric lidar in 2021 and 2022, using RIEGL VQ-880-G II and Teledyne Optech CZMIL SuperNova sensors respectively. The comparisons between these two recent surveys are interesting and informative, whereas the similarities with the 1881 data are more elusive.

I am particularly excited about our third feature which begins on page 26. It's a tutorial rather than an article about a specific project or technology and thus is slanted towards readers new to lidar and those readers working in the field who feel the need for some review. The author is Gottfried Mandlburger, one of the best known lidar teachers and researchers in the modern world. I know Gottfried well. He's now a full professor at the Technical University of Vienna, but I met him when he was spending three years researching at the University of Stuttgart. I've since met him at conferences in several countries and, after much persuasion, he agreed to provide a four-part tutorial on modern airborne lidar. We are very grateful to Gottfried for the considerable work required to create these lessons.

Our fourth feature is from Al Karlin again, this time accompanied by Andrew Peters, both of them with Dewberry. Beginning on page 32, they describe a 20 ppsm lidar survey of the State of Connecticut, flown for the Connecticut State Historic Preservation Office (SHPO). Among the deliverables were LoD2 building models and the key point is that those buildings found from the lidar data to have chimneys in their centers were designated to be historic structures.

LIDAR MAGAZINE

www.lidarmag.com

2024 Vol. 14 No. 4

LIDAR Magazine is published 4x annually by Spatial Media LLC. Editorial mailing address: 7820 B Wormans Mill Road, #236 Frederick, MD 21701. Tel: (301) 668-8887; Fax: (301) 695-1538.

Made in the United States of America

OFFICIAL PUBLICATION

SPATIAL MEDIA

USIBD U.S. Institute of BUILDING DOCUMENTATION

Trimble®

FAST

AS IT GETS

Trimble® mobile mapping systems are designed to integrate seamlessly into your workflow to give you total control from the start all the way through the finish line.

That's the power of Trimble mobile mapping.

DISCOVER MORE AT:
mobilemapping.trimble.com

Not so long ago, there was tremendous debate in the airborne lidar world about linear-mode versus Geiger-mode versus single-photon. Such excitement is characteristic of the geospatial world—I remember animated discussions about opaque versus luminous measuring marks in analytical stereoplotters—and perhaps reflects the Gartner Hype Cycle, but then life goes on. But the subjects of these flurries of conversation remain. On page 36 we present 3DEO, a spin-out from MIT Lincoln Laboratory that makes Geiger-mode lidar systems, both the sensor hardware and the software that optimizes the results. These configurations doubtless had their origins in military systems, but they are operational, and I predict we will hear more from 3DEO. The article is informative, but also educational, because Drs. Kim Reichel-Vischi and Dale Fried explain Geiger-mode principles in an accessible way. There are explanations also in Gottfried Mandlburger's tutorial, so readers have the fruits of three expert's distillations, all in a few pages!

Looking back at 2024

The richness of the end-of-year fare, then, amply underscores the prevalence and persistence of lidar. This is a good time, therefore, to reflect on lidar events in 2024 that I had the privilege to attend. Geo Week 2024 in Denver, marked the last Lidar Leader Awards and the first World Lidar Day (12 February).

The big commercial events, of course, impress with their sheer size and bustle. The Esri International User Conference in San Diego and the INTERGEO conference and trade show in Stuttgart attract just over and just under 20,000 attendees each. There was plenty of lidar content too. INTERGEO is always frustrating: there are three halls with more than 600 exhibitors, so it is impossible to carry out any sort of comprehensive assessment, nor find time for the conference element. Even so, *LIDAR Magazine* had many supberb encounters this year, for example with Trimble (Trimble Applanix president Dr. Steve Woolven is an upcoming podcast guest) and Phase One.

On the Hexagon booth, we learned that more than 700 units of the camera module used in the Leica Geosystems airborne sensors, all of which are modular, have now been fielded. We saw a new hybrid sensor, the usual formula of multiple 150 mp cameras and lidar, with which we are familiar from the CityMapper series, but this time there was great excitement since the new formula is—to be less than scientific—a Leica DMC-4 plus the single-photon lidar sensor from the SPL100. It also transpires that no less than eight SPL100s are in use, collecting data for end-users and for the Hexagon Content Program. This can acquire unbelievable volumes of data.

On the RIEGL booth, we were honored to be conducted through the new products by Dr. Andreas Ullrich—affable, brilliant lidar guru and RIEGL's CTO. The high-end lidar sensor for crewed aircraft appears in its third iteration, the VQ-1560 III-S, which features the integrated data recorder previously seen on the VQ-1460 and a 10% increase in speed from the VQ-1560 II, as well as multiple incremental improvements. The high-end TLS, the long-range VZ-4000i-25, also offers new features. Andreas ended the tour by giving us a potted history of the VUX-1x0 series, from the 120, introduced in 2020, through the 160 (2021), the 180 (2023), to the new VUX-100-25, with a large field of view of 160 degrees and a high pulse repetition rate of up to 1500 kHz.

We enjoyed a memorable visit to the NavVis booth for the launch of the new, handheld MLX sensor, which is smaller, more nimble and less expensive than the shoulder-carried VLX2 and VLX3. The well-orchestrated introduction was led by CEO Dr. Felix Reinshagen, who has subsequently been my guest on *The LIDAR Magazine Podcasts*. Nearby, French UAV-lidar integrator YellowScan was very visible. Their bathymetric Navigator system is going out into the market and the company has successfully adapted to being a manufacturer as well as an integrator. YellowScan's superb user meeting, held near Montpellier, is being repeated biennially, but the company is branching out and is planning regional events around the globe.

Although INTERGEO will run in a similar way for the next three years (in Frankfurt in 2025 and 2027, Munich in 2026), change is afoot. The owner of the event is DVW e.V., the German Association for Geodesy, Geoinformation and Land Management. DVW has chosen Mesago Messe Frankfurt, to take over from the event's current partner, Hinte Expo & Conference GmbH. DVW and Hinte will be continuing their successful working relationship up to and including INTERGEO 2027[1]. From 2028, therefore, we will see changes to the event, as well as a lot more of Frankfurt.

Cheers,

A. Stewart Walker // Managing Editor

1 messefrankfurt.com/frankfurt/en/press/press-releases/2024/intergeo.html

LAStools

LiDAR processing

… fast tools to catch reality

Standalone (Command Line)
Plugins (QGIS, ArcGIS, FME, ...)
Native GUI & Graphical Workbench
Multicore, Batch-Scriptable
Desktop, Server, Cloud
Windows & Linux

52 tools to improve your workflow

Lossless Compression
Transformation & Filtering
Data Conversion
Denoising
Thinning
Indexing
Tiling & Merging
Gridding
Comparing
Normalization
Voxelization

Quality Control
SHP Clipping & Contours
Vectorization
DTM/DSM Generation
Point Classification
Canopy Metrics
Georeferencing
Datum Transformation
Flightline Overage
Coloring
… and many more

Download your trial to get started!

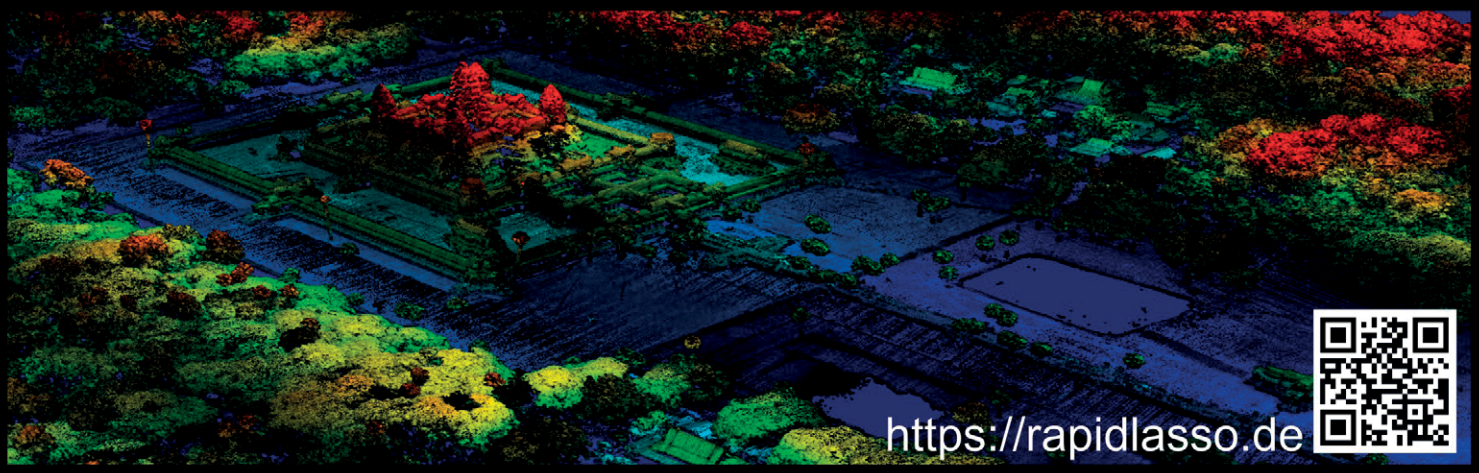

Figure 1: The Anna Lotta Biosphere Reserve is in western Ecuador.

Mapping Green Carbon

How lidar technology is saving Ecuador's tropical dry forests

Among the world's most biodiverse ecosystems, tropical dry forests serve as vital carbon sinks and are teeming with life that supports human existence. However, as environmental changes accelerate, these precious habitats face unprecedented threats. The urgency to understand and manage these issues effectively has never been greater. Enter light detection and ranging (lidar) technology—a revolutionary tool in forest management and conservation.

Lidar has transformed our ability to explore and manage forested regions, offering unparalleled accuracy and detail. This cutting-edge technology has become indispensable for forest managers and environmental researchers. It enables precise biomass estimates, aids in ecological studies, predicts fire behavior, and tracks deforestation patterns, leading to more informed decision-making.

By providing detailed insights into forest structure, composition, and dynamics, lidar-derived information enhances our understanding and facilitates the development of more efficient conservation plans and sustainable land management practices. Moreover,

BY NELSON **MATTIE** AND ALFONSO **GOMEZ**

modeling above-ground biomass with lidar is crucial for evaluating carbon sequestration potential, which is a key strategy in combating climate change.

Lidar is also essential for assessing wildfire risk. Capturing intricate terrain features and forest structures helps predict forest flammability patterns. These data allow fire experts to model fire spread, assess risks, and devise effective fire management and suppression tactics.

Most critically, lidar plays a pivotal role in monitoring deforestation and forest degradation with unprecedented spatial resolution. Providing precise and up-to-date information on land cover changes supports efforts to combat illegal logging, land conversion, and other drivers of deforestation, thus contributing significantly to global forest preservation initiatives.

In this groundbreaking conservation project, we utilized full-waveform lidar data to map Ecuador's tropical dry forests. By deploying the RIEGL LMS-Q680i airborne laser scanner, aerial photography, AI algorithms, and sophisticated software from suppliers such as rapidlasso (LAStools) and BayesMap Solutions, we combined cutting-edge technology with advanced data processing methods, including machine learning algorithms for data analysis and regression. This represents a major leap forward in our ability to understand, manage, and protect invaluable forest ecosystems.

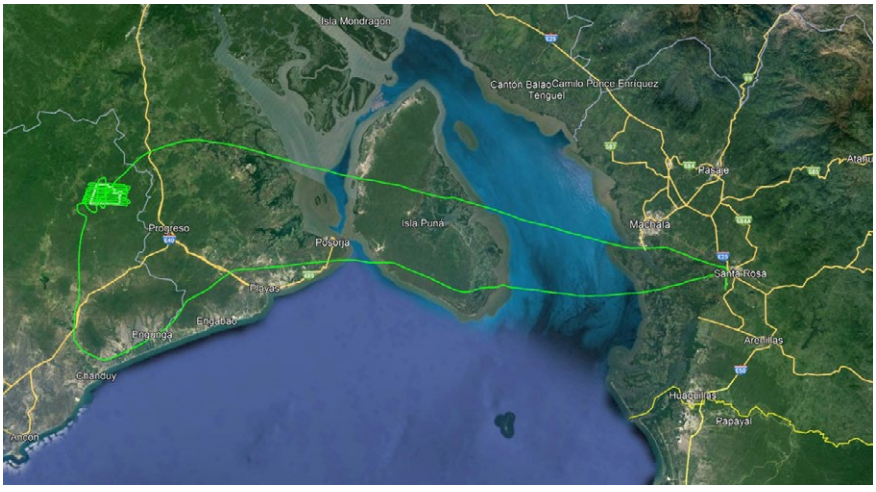

Figure 2: Flight path carried out above the Anna Lotta Biosphere Reserve.

Figure 3: The RIEGL LMS-Q680i system was mounted on a Cessna 206 airplane. The sensor operates at a wavelength of 1550 nm and was set to 400 kHz. The flight was conducted at an altitude of 700 m above ground level, with an average speed of 85 knots.

The Anna Lotta Biosphere Reserve: a sanctuary under threat

Perched along Ecuador's Pacific coast lies the Anna Lotta Biosphere Reserve (**Figure 1**), a region characterized by xerophytic ecosystems, including increasingly rare tropical dry forests. These forests have suffered a staggering loss of over 70% of their original extent and face severe threats from climate change and human activity. Located in Ecuador's most densely populated region, these forests are in the area most affected by climate change and have undergone severe drought periods, as reported by

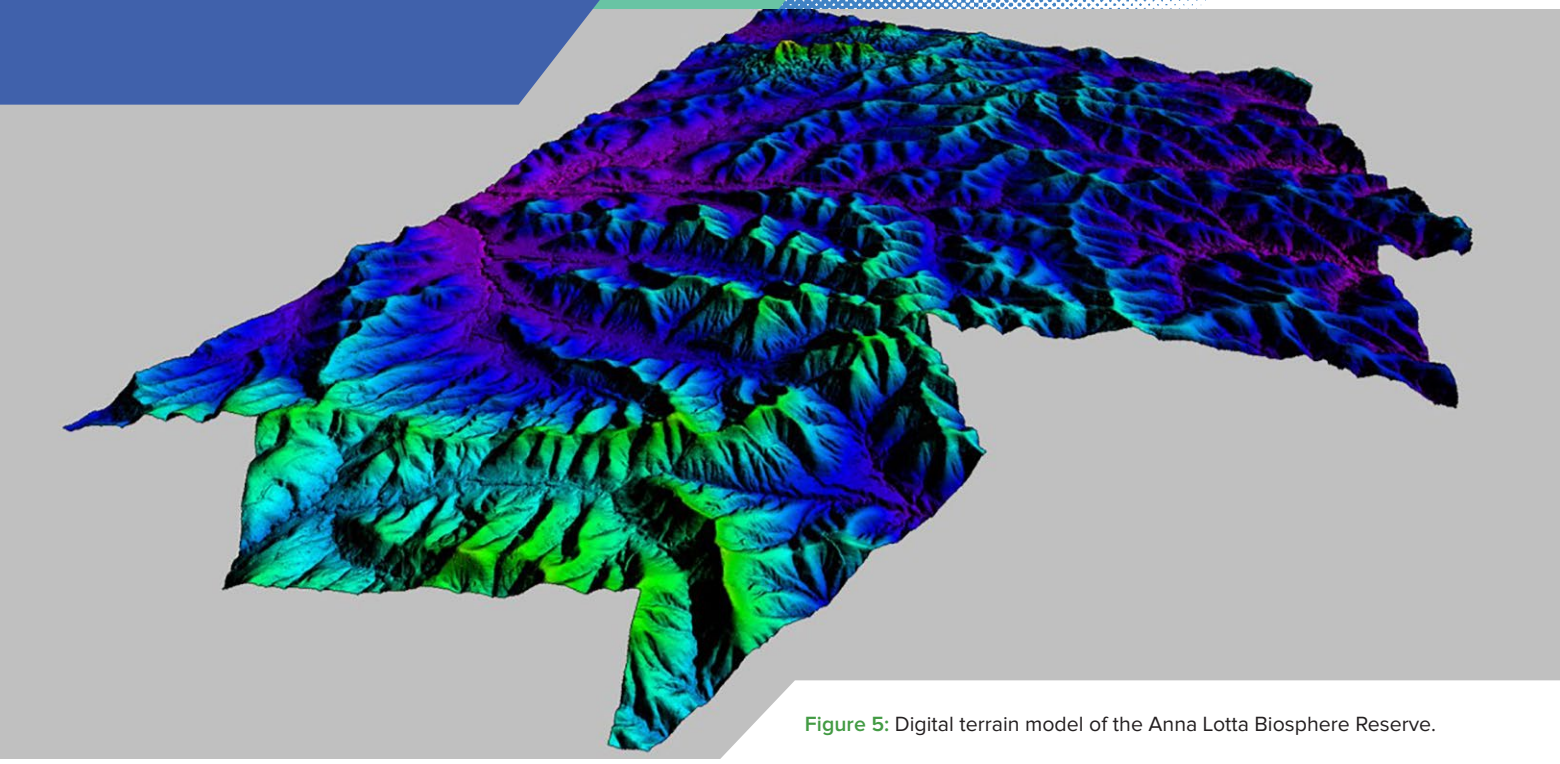

Figure 5: Digital terrain model of the Anna Lotta Biosphere Reserve.

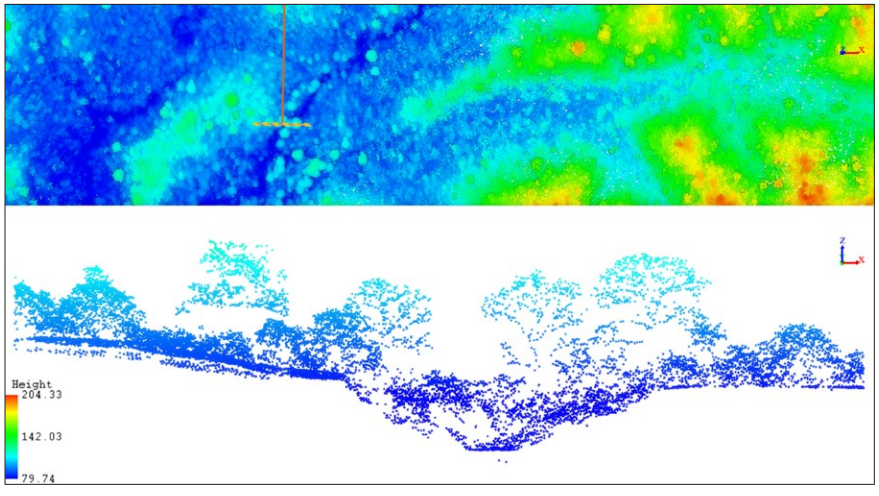

Figure 4: Vertical profile of a tropical dry forest in the Anna Lotta Biosphere Reserve.

Ecuador's Ministry of Environment, Water, and Ecological Transition.

Globally, tropical dry forests are among the most endangered ecosystems, surpassing tropical rainforests in terms of vulnerability. In Ecuador, rampant degradation and deforestation have led to significant fragmentation, necessitating new protective measures and vigorous monitoring of land use changes.

Our project area encompasses tropical dry forests on Ecuador's southern coastline within the Tumbesian-endemic zone. These forests are in a better state of preservation than those on the central and northern coasts of Ecuador and northern Peru. Renowned for their intricate ecological interactions and immense environmental importance, these forests are a focal point in the fight against climate change.

The main purpose of the Anna Lotta Biosphere Reserve is to safeguard and maintain tropical dry forests within this privately held woodland in Ecuador for enduring carbon sequestration and biodiversity conservation. Its climate-related aim is to prevent emissions from deforestation and degradation.

Since 2007, the reserve has been under the stewardship of its proprietor, Dr. Jaime Rocero Maquilón, a German-Ecuadorian physician who is deeply committed to environmental preservation. Dr. Rocero's vision extends beyond merely conserving the forest and aims to inspire similar initiatives across Ecuador. By leveraging carbon credits to improve forest management, he plans to fund ongoing biodiversity conservation efforts and enhance the ecological health of the area.

Carbon funding will support crucial maintenance tasks, such as introducing local tree species for restoration, improving fencing, and enhancing surveillance and monitoring. Additionally,

Versatility at its finest.

A one-of-a-kind laser scanner

The YellowScan Explorer can be mounted on a light manned aircraft or switched to different types of UAV platforms. Combined with 1-year unlimited technical support and training, our users will be ready to take full advantage of Explorer's functionality and successfully complete their surveying projects.

Discover it now!

- yellowscan.com
- contact@yellowscan.com
- +1 801 876 1007

YellowScan

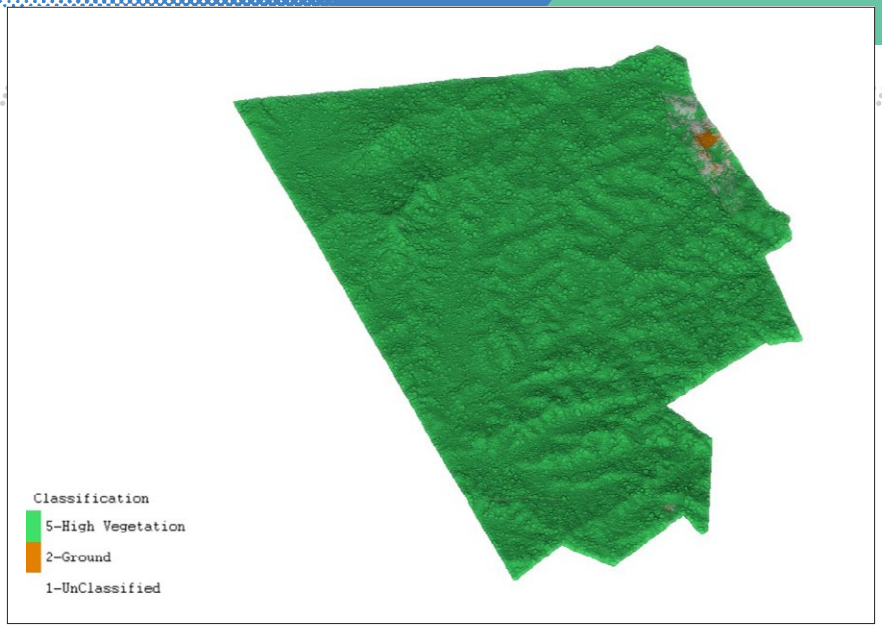

Figure 6: Classified lidar point cloud of Anna Lotta Biosphere Reserve.

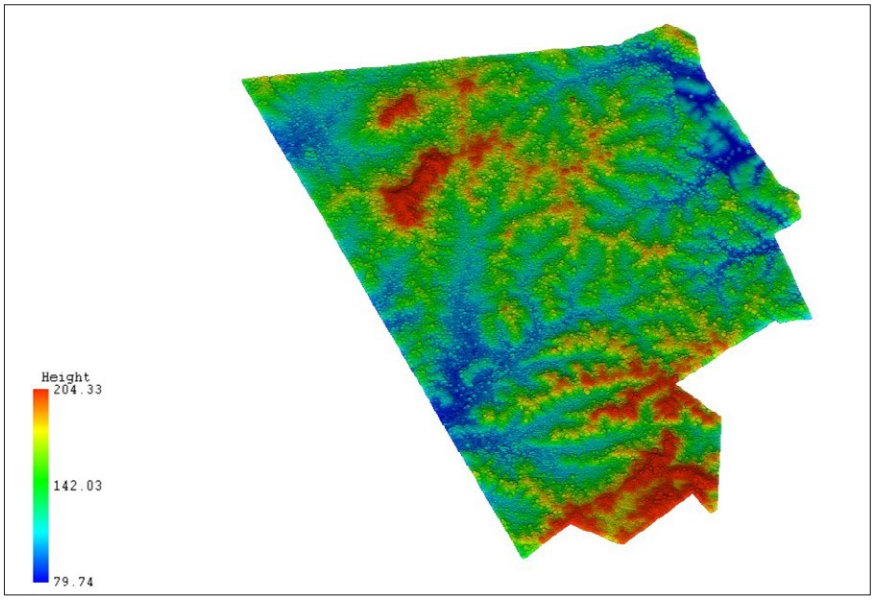

Figure 7: Lidar point cloud of Anna Lotta Biosphere Reserve.

it will support environmental education programs for nearby communities and other vital activities.

Green carbon mapping: a technological leap

In January 2024, our team embarked on a mission to capture detailed data over the Anna Lotta Biosphere Reserve using a RIEGL LMS-Q680i sensor, an airborne laser scanner designed for long-range applications. This state-of-the-art equipment is particularly effective for aerial surveys in varied terrains, making it ideal for mapping intricate landscapes of the reserve. Moreover, it helped us to create a faithful and accurate record of the existing forest, which will serve as a baseline for monitoring this area in the coming years.

The dataset we analyzed contained full-waveform lidar data collected from a single flight over the reserve (**Figure 2**). Acquired by Stereocarto, a leading geospatial services company operating in Europe and Latin America, the data provided a wealth of information about forest structure and composition.

The RIEGL LMS-Q680i boasts advanced features, including a powerful laser source, multiple-time-around (MTA) processing, and digital full-waveform recording (**Figure 3**). These attributes allow efficient operation in Ecuador's challenging environments by capturing data with remarkable precision.

Why full-waveform lidar?

Utilizing full-waveform lidar data brought numerous benefits to our project (**Figure 4**):

- **Enhanced analysis of vegetation structure**: Full-waveform lidar captures the complete reflected signal, offering detailed insights into the vertical structure of vegetation, from the canopy and sub-canopy to branches, trunks, understory, and ground surface. This enables a more precise evaluation of forest biomass and vegetation layers.
- **Improved ground identification**: Since the entire waveform of the laser pulse is recorded, it becomes easier to differentiate between the forest canopy and the ground, even in densely vegetated regions.
- **Higher point density**: Full-waveform lidar data often result in a greater density of data points, enhancing the resolution and intricacy of the collected data. This is particularly advantageous for detecting small features and changes within the forest.

GEO WEEK

FEBRUARY 10-12, 2025
DENVER, CO - USA
geo-week.com

The intersection of
geospatial +
the **built world**

Accomplish a year's worth of geospatial business in just one week by attending Geo Week 2025

Geo Week is the premier event for the built world and geospatial professionals, created in response to the increasing convergence of technology in today's world. Geo Week's conference program and tradeshow floor feature commercial applications of 3D technologies, innovations, and case studies in the built environment, advanced airborne and terrestrial remote sensing solutions, smart products for an entire project team, and much more! Experience the future at Geo Week.

INDUSTRIES SERVED

- Architecture, Engineering & Construction
- Asset & Facility Management
- Disaster & Emergency Response
- Earth Observation & Satellite Applications
- Energy & Utilities
- Infrastructure & Manufacturing
- Land & Natural Resource Management
- Mining & Aggregates
- Surveying & Mapping
- Urban Planning & Smart Cities

REGISTER AT GEO-WEEK.COM
Use code **SAVE100** for $100 off a conference pass or a **FREE** exhibit hall pass.

PRESENTED BY: GEO WEEK NEWS

CONFERENCE AND EVENT PARTNERS: asprs THE IMAGING & GEOSPATIAL INFORMATION SOCIETY, RCN

EVENT PARTNERS: asprs, isprs, MAPPS, RCN, USIBD, USGIF 20TH ANNIVERSARY, World Geospatial Industry Council

Produced by diversified

Figure 8: Aerial RGB photograph of Anna Lotta Biosphere Reserve at 5 cm/pixel resolution.

Figure 9: Field forest inventory conducted at the Anna Lotta Biosphere Reserve.

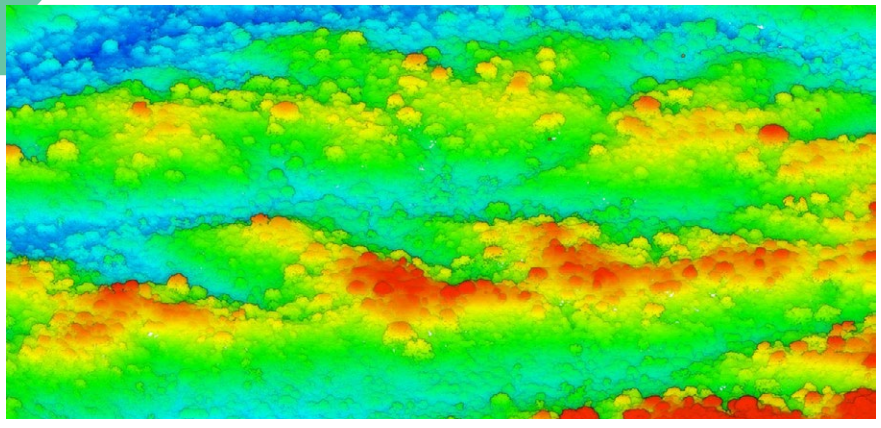

Figure 10: Detailed forest mapping in the Anna Lotta Biosphere Reserve using lidar point-cloud technology.

- **Enhanced object categorization**: The additional information from full-waveform lidar aids in distinguishing between various types of vegetation and other objects in the forest, leading to more precise classification and mapping.
- **Penetration through thick canopy**: Full-waveform lidar is more efficient at penetrating dense canopies and capturing data from multiple layers within the forest—a crucial capability for examining forests with thick vegetation where traditional lidar methods may struggle.
- **Increased precision in biomass estimation**: The detailed vertical profiles and forest metrics acquired from full-waveform lidar enhance the precision of biomass estimation, which is essential for ecological research and forest management.
- **Improved detection of understory vegetation**: Full-waveform lidar excels at detecting and characterizing understory vegetation and provides vital information for fire behavior and combustibility modeling, biodiversity research, and habitat assessment.

Unveiling the forest's secrets

In this groundbreaking study, our team harnessed advanced lidar technology and machine learning algorithms to map and analyze the Anna Lotta Biosphere Reserve. The project not only produced a highly detailed topographical survey of the reserve (**Figure 5**), but also offered crucial data on biomass and carbon stock estimations, underscoring the importance of innovative technologies in environmental conservation.

We collected full-waveform lidar data over the 2500-hectare reserve, processing it with tools such as LAStools and BayesMap WavEx, alongside machine-learning algorithms in the R programming language. This approach allowed for an unprecedented level of detail in capturing the forest's structure and composition.

The data was projected using the WGS84/UTM zone 17S coordinate system, with elevations adjusted via the EGM2008 geoid model to ensure precise height measurements.

We collected approximately 1.62 billion laser point records, adhering to LAS specification version 1.4. Due to the dense forest coverage, the majority of these points, 620 million, were first returns. We achieved a high point density of 30.35 points per square meter (ppsm) for all returns and 11.62 ppsm for last returns only—essential for accurate ground surface modeling (**Figure 6**).

The intensity values of the laser returns ranged from 0 to 25,827, indicating varied surface reflectivity within the forest environment. Elevation values spanned from 58 to

235 m, reflecting the reserve's complex topography and diverse vegetation (**Figure 7**).

Ensuring data accuracy

To guarantee the accuracy of the dataset, we conducted comprehensive quality control using rapidlasso's LAStools QC capabilities and BayesMap Solutions' FastQC tools. This process involved generating detailed raster images that enhanced data analysis and pinpointed potential issues. The following quality control measures were key:

- **Time intervals and overlap maps**: Automated determination of high-frequency IMU drift correction intervals and visualization of overlapping swaths are critical for accurate registration.
- **Relative time deviation plots**: Identification of self-overlap issues and multi-channel mixing ensured precise timestamp mapping.
- **Roughness maps**: Visualization of terrain properties aided in understanding vegetation types and natural terrain features.
- **Height maps**: Provided essential elevation data for further analysis.
- To correct the initial data inaccuracies, we used BayesMap Solutions' strip-alignment feature to fix significant misalignments and systematic errors. The strip alignment process involved several key steps:
- **Quality checks before and after alignment**: Ensured data consistency and integrity throughout the process.
- **Data tiling and gridding**: Organized the data into manageable sections for efficient processing.
- **Projection and geometry validation**: Synchronized and validated the dataset's geometry to ensure spatial accuracy.
- **Optimal correction calculations**: Adjusted misalignments based on registration results to refine the dataset.
- **Generating visual metrics**: Vector images and statistical outputs were created to assess the effectiveness of the corrections.
- **Producing corrected files**: Generated a fully corrected LAS/LAZ dataset ready for application.

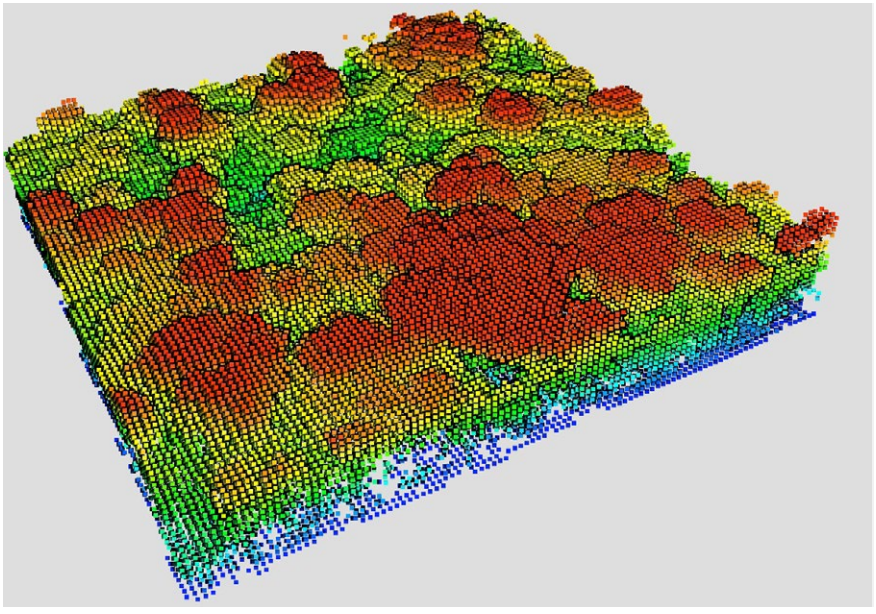

Figure 11: Voxelization of lidar point cloud in Anna Lotta Biosphere Reserve.

After applying these corrections, the root-mean-square (RMS) residual vertical error was impressively reduced to 0.055 m. This significant improvement demonstrates the effectiveness of the correction methods and highlights the crucial role of advanced data extraction and processing algorithms for aerial lidar data.

Revealing new insights

Our study (**Figures 8, 9 and 10**) revealed differences in biomass and carbon storage between the Anna Lotta Biosphere Reserve and the official Ecuadorian national averages for tropical dry forests, highlighting the importance of site-specific data.

While the National Forest Inventory reports an average basal area of 9.1 m^2 per hectare, a volume of 53.9 m^3 per hectare, and carbon storage of 37.0 megagrams of carbon per hectare (Mg $C{\cdot}ha^{-1}$), the Anna Lotta Biosphere Reserve field forest inventory showed a basal area of 8.2 m^2 per hectare, a volume of 49.11 m^3 per hectare, and higher carbon storage at 44.34 Mg $C{\cdot}ha^{-1}$.

Using lidar data and support vector machine (SVM) regression models, we estimated the above-ground biomass (AGB) for the reserve at 104.42 Mg ha^{-1}, with a carbon stock of 49.08 Mg $C{\cdot}ha^{-1}$ and an equivalent carbon dioxide sequestration of 180.12 Mg CO_2 per hectare. These findings emphasize the reserve's unique characteristics and

demonstrate how advanced technologies can provide more accurate and localized environmental data.

From voxelization to forest digital twins

A key aspect of our project was the voxelization of tropical dry forests (**Figure 11**) and the generation of a forest digital twin (FDT). What is the difference between a voxelized forest model and FDT?

A voxelized forest model is a static, three-dimensional representation in which the forest space is divided into small cubic units called voxels. Each voxel contains detailed information about the physical characteristics at a specific location, such as vegetation density, canopy height, and biomass distribution. This model focuses primarily on capturing the structural complexity and spatial attributes of the forest at a specific point in time, aiding in morphological analyses, and contributing to biomass estimation and carbon-balance studies.

In contrast, an FDT is a dynamic, multidimensional virtual replica of a forest ecosystem that goes beyond mere structural representation. An FDT integrates structural data with ecological processes, temporal dynamics, and biological interactions, continuously updating real-time data from various sources, such as aerial or terrestrial sensors and satellite data.

Conclusion: a technological beacon for conservation

This pioneering work in the Anna Lotta Biosphere Reserve showcases the transformative power of combining cutting-edge lidar technology with sophisticated data processing and machine learning techniques. By providing a more nuanced and accurate picture of forest biomass and carbon stocks, our study not only advances scientific understanding but also equips policymakers and conservationists with the tools necessary to make informed decisions in the fight against climate change.

Additionally, this initiative contributes to the production of high-quality carbon credits, enhancing the credibility of climate pledges. Each issued credit signifies a verified ton of carbon removal. By providing complete transparency and monitoring the process using the most reliable data for independent verification, we guarantee that stakeholders can rely on the genuine climate impact. Entrusting precise measurements to experts ensures that project contributions result in tangible and quantifiable environmental advantages.

As we continue to refine these technologies and methodologies, we will move closer to a future where we can monitor and protect our planet's most vulnerable ecosystems with unprecedented precision. The Anna Lotta Biosphere Reserve is a testament to what can be achieved when innovation meets dedication in the pursuit of environmental conservation.

With over two decades of geospatial expertise, **Nelson Mattie** specializes in remote sensing and is affiliated with organizations such as SELPER, CRSS, ASPRS, and IEEE GRSS. He holds degrees from institutions in Venezuela, the United States, Spain, Italy, Costa Rica, and Chile, and is pursuing his Ph.D. at the University of Alberta's Center for Earth Observation Sciences. in Canada. His research involves advanced lidar technologies, such as NASA's GEDI, and explores quantum computing and AI applications. Nelson focuses on forest ecology, biomass estimation, fire behavior analysis, and the quantification of global green and blue carbon reserves, contributing significantly to forest management and biodiversity conservation. He also collaborates with lidar Latinoamerica LLC on over 100 projects in 19 countries across sectors such as forestry, mining, agriculture, oil and gas, and infrastructure.

Alfonso Gómez has dedicated his career to entrepreneurship, education, and innovation, merging academia with active private sector roles. He is a tenured professor in the School of Agricultural Engineering at the Polytechnic University of Madrid. Within the university, he is part of the Department of Cartographic Engineering, Geodesy, Photogrammetry, and Graphic Expression in Engineering. For nearly 30 years, he has led Stereocarto in general management and commercial capacities, driving its national and international growth, and making it a geospatial engineering benchmark. He has also helped create complementary businesses to strengthen Stereocarto's consolidation and expand its European and Latin American presence, serving governments, public and private enterprises, and engineering firms that require spatial data for decision-making. From the outset, Alfonso has researched new geographic information methods and applications, leading significant innovation projects in territorial knowledge and management, solidifying his leadership in the field.

References

RIEGL Laser Measurement Systems: www.riegl.com

BayesMap Solutions software: https://bayesmap.com/products/bayeswavex/

rapidlasso LAStools software: https://rapidlasso.de/

R Programming language: https://www.r-project.org/

Stereocarto: www.stereocarto.com

lidar Latinoamerica: https://www.lidarlatinoamerica.com/

Carlson Software for
Photogrammetry + LiDAR
Bridging the Gap Between UAVs and CAD

Carlson PhotoCapture

- Choose a perpetual license or cloud-based pay-as-you-go model
- Accuracy through control points, full RTK UAV support, LiDAR integration
- Output point clouds, volumes, surfaces, elevations, and more
- 30-day free trial

Powerful, versatile, scalable photogrammetry processing. **Online or standalone.**

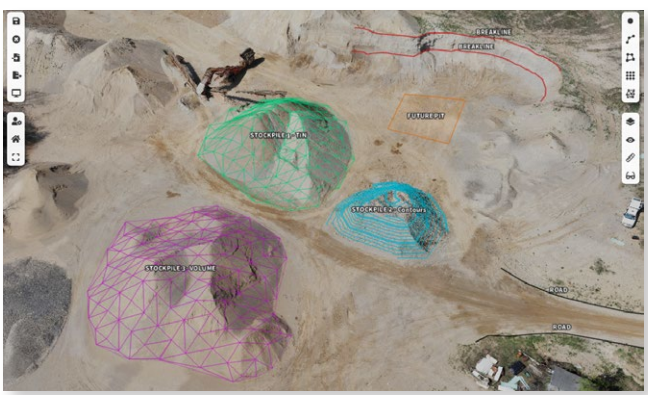

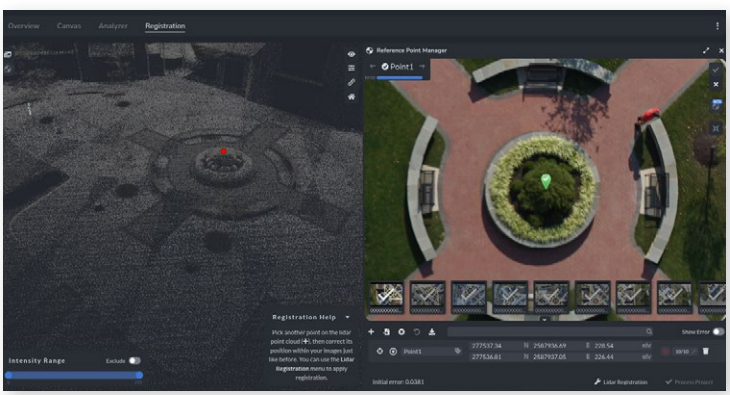

- Sparse or Dense point clouds
- Orthoimages
- Digital Elevation Models
- Project Quality Reports
- Survey Canvas – Virtual Drafting
- Calculate distances, areas, and volumes
- Create points, linework, grids, TINs, and contour lines
- Export in a wide variety of file formats

- Powerful tools such as bare earth and feature extraction
- Point clouds to finished plats
- Point clouds to profiles & sections
- Polylines to CAD

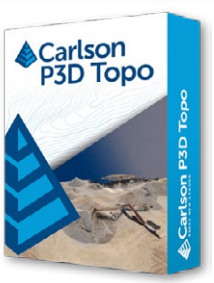

- Powerful point cloud editing in a 3D environment
- Pit/pile volumes
- Surfaces to CAD

Learn more at carlsonsw.com/photogrammetry
33 East 2nd Street ■ Maysville, KY 41056, USA
800-989-5028 ■ 606-564-5028 ■ www.carlsonsw.com

Carlson
BREAK NEW GROUND

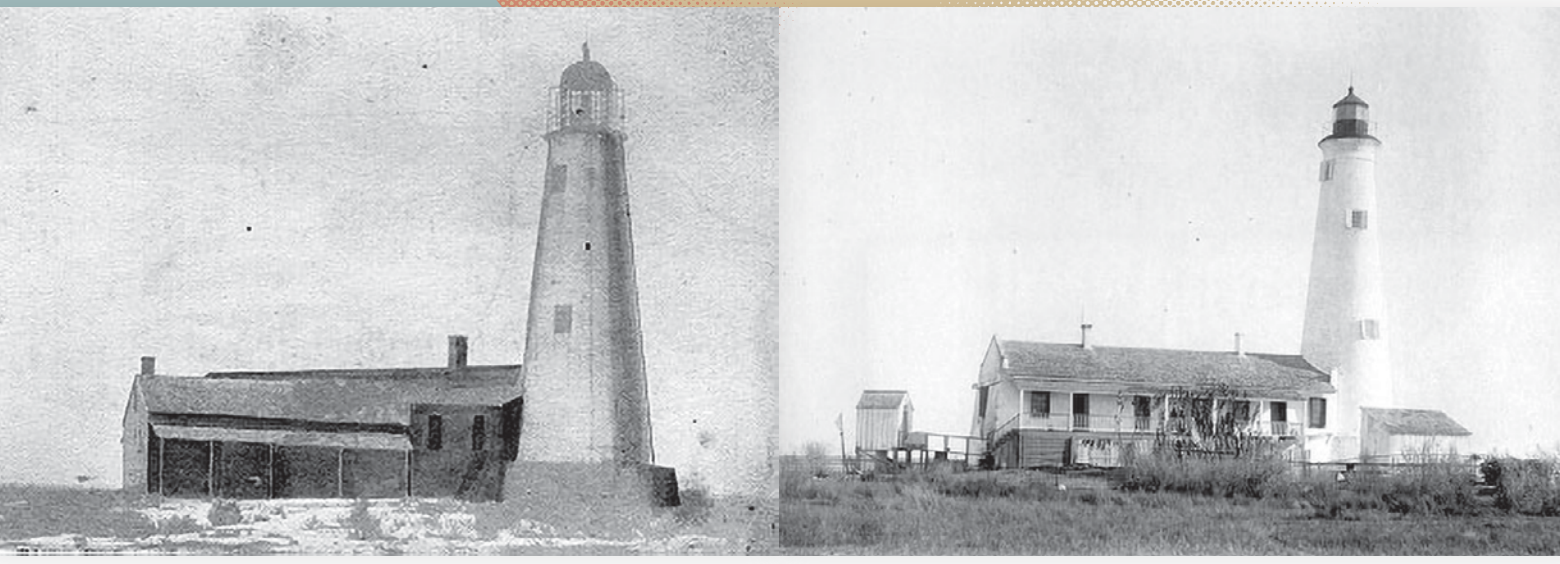

Two historic US Coast Guard photos, from 1831 (left) and 1842 (right), showing the St. Marks Lighthouse (the likely landmark used originally to position the Ochlockonee Shoal) as it would appear when viewed from the shoal, approximately 10 miles to the south.

Century-Old Maps of Ochlockonee Shoal Updated with Topobathymetric Lidar

New survey combats dangers to shipping in Florida's Big Bend

Figure 1: General location map of the Ochlockonee Shoal, east of Alligator Harbor in Franklin County, Florida.

A pronounced shallow area, known as the Ochlockonee Shoal, lies in the Gulf of Mexico about eight miles off the Big Bend of the Florida shoreline. The shoal is located at the confluence of the pre-historic channels of the Ochlockonee, St. Marks, and Aucilla Rivers (**Figure 1**). The shoal is believed to have been a topographic rise near that confluence during the last glacial maximum when the coastline itself was many miles seaward of its current location (Cole, 2021). As sea level rose during the last 15,000 years, the rise is believed to have become an offshore island. Then, based on the

BY AL **KARLIN** AND GEORGE **COLE**

SBG SYSTEMS

High-Performance INS Solutions for Surveying Applications

NEW QUANTA SERIES

- Designed for Seamless OEM Integration
- Robust to Vibrating Environments
- Post-processing with Qinertia PPK Software

Quanta Micro

Quanta Plus

Quanta Extra

l.ead.me/lidarmag

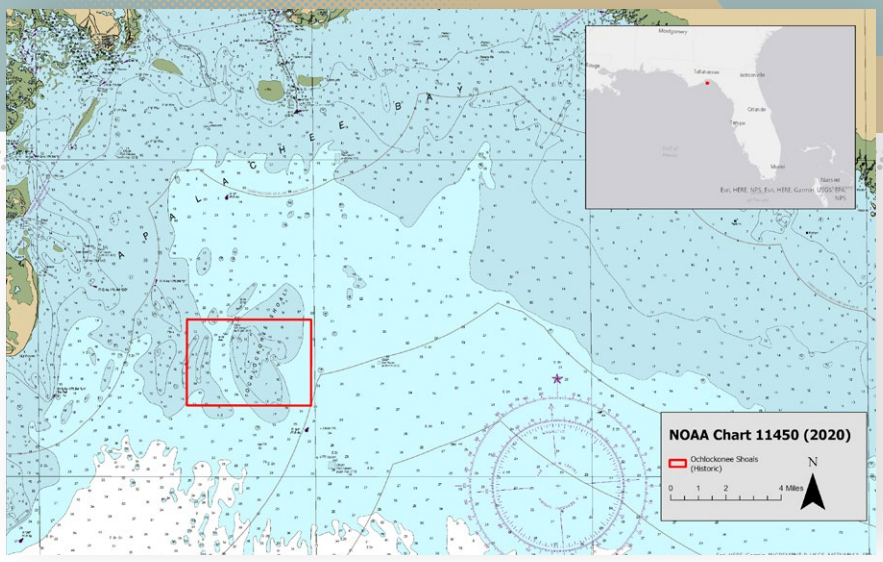

Figure 2: The Ochlockonee Shoal as shown on NOAA Nautical Chart 11450 (2020).

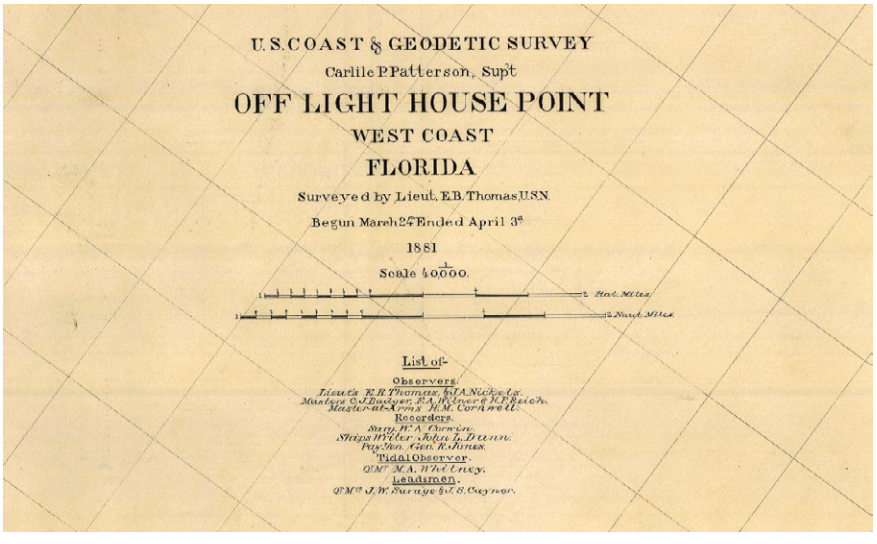
U.S. COAST & GEODETIC SURVEY

Carlile P. Patterson, Supt

OFF LIGHT HOUSE POINT

WEST COAST

FLORIDA

Surveyed by Lieut. E.B. Thomas U.S.N.

Begun March 24 Ended April 3d

1881

Scale 1/40000

Half Miles

Quarter Miles

List of-

Observers.

Lieuts R.R. Thomas, and A. Nicholas

Masters C.J. Badger, E.A. Driver & H.P. Leach.

Master-Assts Wm. M. Cornell.

Recorders.

Surg. W.A. Curtin.

Sheip Writer John L. Dunn.

Pay Mas. Gen. R. Symes.

Tidal Observer.

QMr M.A. Whitney.

Leadsmen.

QMrs J.W. Savage & U.S. Cagwin.

Figure 3: Title caption from 1881 U.S. Coast and Geodetic Survey draft chart (HO1489).

generally accepted rate of post-glacial sea-level rise (Basillie and Donaghue, 2011; Holmes, 2011), the shoal became completely submerged about 8000 years ago. The shoal appears on current National Oceanic and Atmospheric Administration (NOAA) nautical charts as having a least depth of three feet above mean lower low water (**Figure 2**).

The shoal and similar obstructions along the Gulf Coast have a long history of being a threat to shipping. The Spanish created a mission in the area north of St. Marks about 1633 to exploit the agricultural expertise and labor of the Apalachee Native Americans with the goal of alleviating the chronic food shortage at the St. Augustine colony. The mission soon began producing an abundance of corn and other crops, but the hazardous sea voyage through the shoals near the mission prevented transport to St Augustine on ships. To resolve this, the Spanish governor sent a hydrographic surveyor to the area to map a safe route through the shoals. Unfortunately, no record of that survey work has yet been found. Nevertheless, in 1639, the first Spanish *fragata*, loaded with corn and other produce from the new mission, successfully made the 800-mile trip, past the Ochlockonee Shoal and around the Florida peninsula, to rescue the starving St. Augustine colonists.

After Spain ceded the Florida Territory to the United States in 1821, the shoal continued to be a hazard to shipping. Prior to the extension of railroads to the area, the shoal was along the shipping route for cotton and other agricultural products from the Red Hills area of North Florida. Then, during the Civil War, when President Abraham Lincoln ordered a blockade of the Confederate coastline, the U.S. Navy squadron guarding the Gulf experienced great difficulty in patrolling the Big Bend area because of shoals (Cole and Ladson, 2020). As a result, the area became a favorite of ships trying to run the blockade, as well as for Confederate salt production.

Owing to the problems experienced during the Civil War, Congress requested the Coast and Geodetic Survey (C&GS) unit to map the shoal. As a result, in 1881, C&GS mapped the shoal (**Figure 3**), under the direction of Lt. E.B. Thomas. The resulting draft chart was eventually published two years later (Chart LC00182; **Figure 4**.)

Research into the history of the hydrographic data used to compile the current chart (**Figure 2**) indicates that sounding and depth contours around the shoal were based solely on the hydrographic survey (U.S. Coast & Geodetic Survey HO1489) conducted in 1881 (**Figures 3 and 4**). Although the descriptive report for the survey is not available, the soundings for that survey would have used a lead-weighted line for measuring depths and some type of visual positioning process, such as horizontal sextant measurements, for establishing the geographic positions of the soundings.

LP360 DRONE

Wingtra LIDAR is now supported by LP360!

The latest updates in LP360 can take your data to the next level.

Are you using the new Wingtra LIDAR Solution to capture 3D data for large aerial surveying projects? Then take that data to the next level with LP360 Drone LiDAR & photogrammetry 3D point cloud software.

With LP360 Drone you can process, analyze, and maximize your Wingtra LiDAR survey data, creating enhanced and highly accurate deliverables.

The fully integrated workflow of LP360 Drone lets you Fly, Optimize and Deliver fully processed data into actionable results. Learn how you can get the most out of your Wingtra LiDAR with LP360 Drone.

Get the most out of your Wingtra LiDAR Data with LP360 Drone

- Manage your coordinate system (geoid, grid to ground, local site, datum and epoch change)
- Leverage LP360 powerful 3 synchronized viewing windows and Image Explorer tool
- QC/QA your data with Automatic Ground Control Detection and 3D Correction
- Access all the other advanced tools such as Smoothing, Automated Outlier Removal, Automatic Classification, Break lines, DTM and Contour Generations, export to CAD formats, volumetric calculations, powerlines encroachment tools and much more
- Customize / define your own workflow with the new GUI
- Go further with unique LP360 Cloud Extension (optional add-on) to store, search, share and stream your data with any LP360 Desktop

Scan to learn more >

SPECIAL OFFER!

Get LP360 Cloud to Make Your Geospatial Work Easier

RIGHT NOW, for any LP360 order, get **3 months of FREE access** to LP360 Cloud and Cloud Starter

LP360 Cloud is an ever-growing collection of cloud-based tools and resources that will make it easy for you to manage, archive, share and collaborate on geospatial projects.

LP360 Cloud is an ever-growing collection of cloud-based tools and resources that will make it easy for you to manage, archive, share and collaborate on geospatial projects.

- Store and manage data
- Stream pointclouds
- Discover Powersearch to localize all available datasets within a geographical area

	RIEGL VQ-880-G II	Teledyne Geospatial CZMIL SuperNova
Date of survey	22 December 2021	4-6 November 2022
Resolution/Density	Average 6 pulses/m^2	Average 6 pulses/m^2
Nominal pulse spacing	0.41 m	0.41 m
Survey altitude (AGL)	400 m	400 m
Scan frequency	80 lines per second	Proprietary
Target pulse rate	200 kHz	Proprietary
Pulse length	1.5 nanoseconds	Proprietary
Central wavelength(s)	532 nm	532 nm; 1064 nm
Accuracy		
RMSEz (Non-Vegetated; 95th percentile)	≤ 10 cm	N/A
NVA (95% confidence level)	≤ 19.6 cm	5.1 cm
BVA (≤ 30 cm)	N/A	28.2 cm
Flightline direction	East-West	North-South (Diagonal)
Project	ARI	NOAA/NGS
Coordinate reference system	Florida State Plane North	UTM17
Datum	NAD 1983/2011	NAD1983/2011
Horizontal units	U.S. foot	m
Vertical units	U.S. foot	m

Table 1: Specifications for topobathymetric lidar surveys of the Ochlockonee Shoal area.

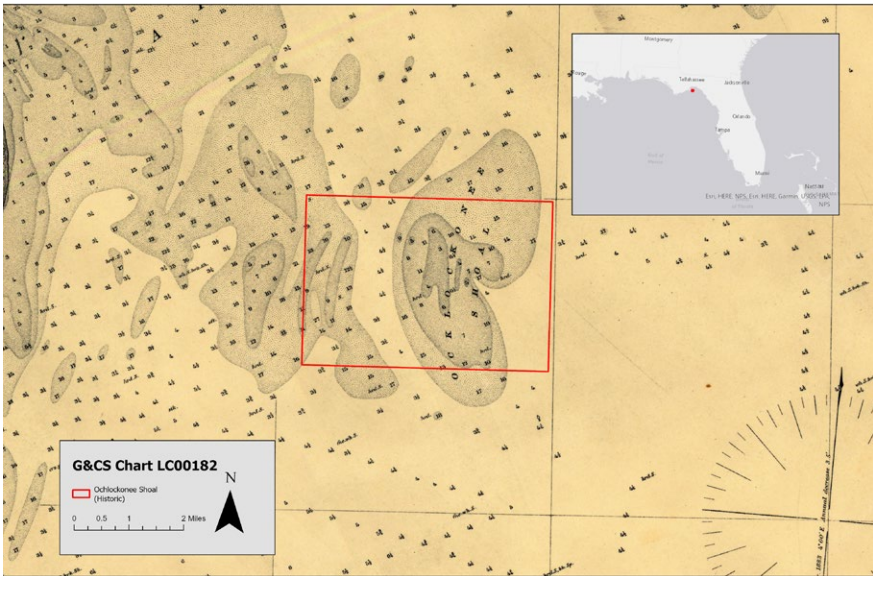

Figure 4: The Ochlockonee Shoal as originally published on NOAA (C&GS) Nautical Chart LC00182 (1883).

From Chart LC00182 (**Figure 4**), it is clear that the 1881 C&GS survey measured only four sounding lines across the shoal, none of which sampled its apparent geometric center. The sparse survey of the shoal, in combination with the absence of any subsequent and/or newer NOAA records, suggests that very little hydrographic information was collected regarding the shoal during the 140-year span between 1881 and 2021.

Recent topographic lidar surveys

Due to the lack of data for the shoal and the potential for it to contain priceless archaeological, historical and geologic information, the Aucilla Research Institute (ARI), a private non-profit research institute, contracted for a bathymetric lidar mapping of the shoal using grant funding from the Florida Division of Historic Resources and the Ingals Foundation. Unfortunately, the funding was insufficient to map the entire shoal area. NV5 Geospatial was contracted to acquire and process the lidar data. The area of interest (AOI) (**Figure 5**) was surveyed on December 22, 2021 using a RIEGL VQ-880-G II topobathymetric lidar sensor.

In 2022, however, NOAA/NGS (National Geodetic Survey) tasked Dewberry to map a much larger area in the Big Bend, including the ARI/NV5 lidar footprint (turquoise area in **Figure 1**). This NOAA/NGS mapping was performed on November 4-6, 2022 using a Teledyne Geospatial Coastal Zone Mapping and Imaging Lidar (CZMIL) SuperNova topobathymetric lidar sensor. **Table 1** compares the technical specifications of the two surveys.

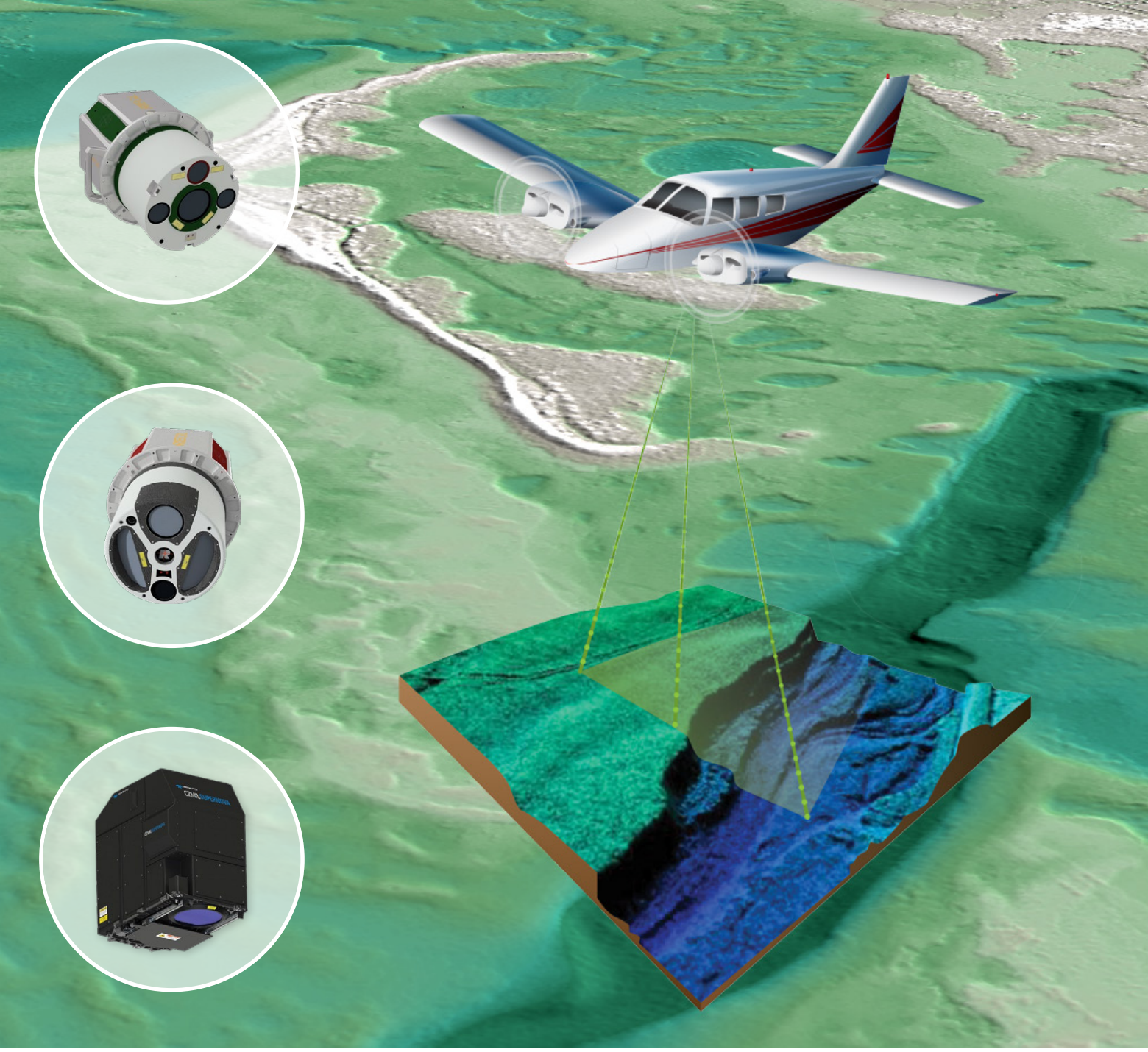

APPLYING THE LATEST TURNKEY SOLUTIONS AND REMOTE SENSING TECHNOLOGY **FROM DATA ACQUISITION TO CLIENT DELIVERY**

Jason Dolf, CP, CMS
jdolf@dewberry.com
813.327.5069

Dewberry
www.dewberry.com

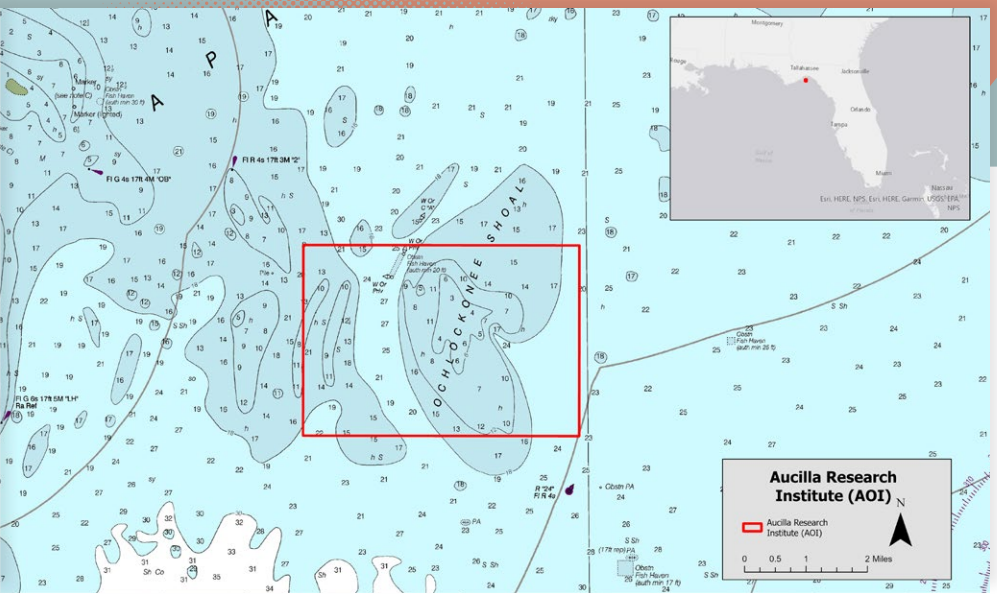

Figure 5: Aucilla Research Institute/NV5 (2021) Ochlockonee Shoal topobathymetric area of interest.

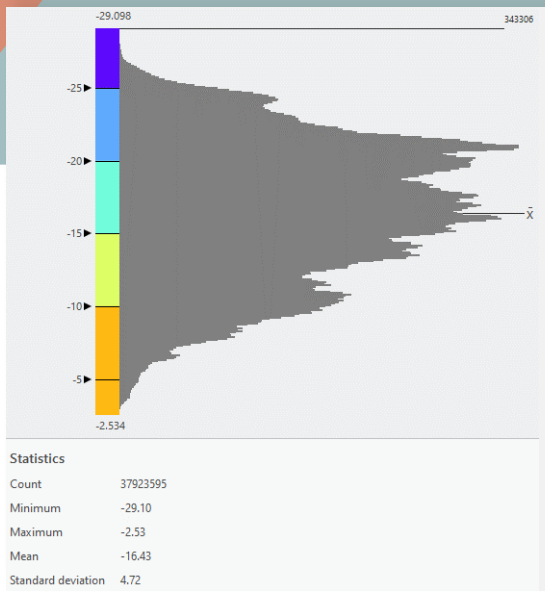

Figure 6: Depth response distribution from the VQ-880-G II sensor.

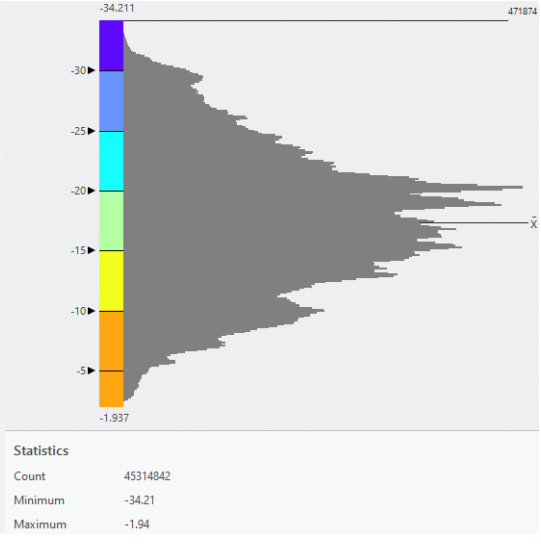

Figure 7: Depth response distribution from the CZMIL SuperNova sensor.

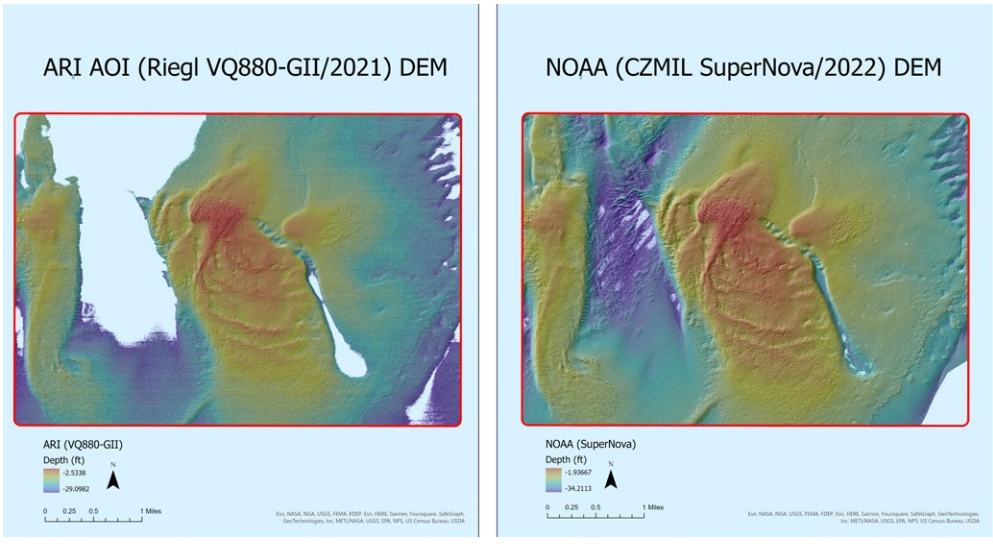

Figure 8: Comparison of the ARI/VQ-880-G II DEM (left) and the NOAA/CZMIL SuperNova DEM (right). Both DEMs are shown as a 5X exaggerated hillshade raster.

Lidar deliverables

In addition to the classified (ASPRS bathymetric classification) lidar point clouds, deliverable products from both the 2021 and 2022 surveys included: topobathymetric bare earth digital elevation models (DEMs), normalized intensity images, and vector representations of the flightlines, project boundary, and ground surveys. One-foot topobathymetric contours were generated from the DEMs. Portions of the 2021 survey are available directly from ARI; the 2022 survey products are available on the NOAA Digital Coast data viewer (https://www.coast.noaa.gov/dataviewer/#/).

Comparison between the two lidar sensors

Both the RIEGL VQ-880-G II and the Teledyne Optech CZMIL SuperNova are considered to be state-of-the-art topobathymetric sensors by the airborne lidar community. While the VQ-880-G II is a single frequency sensor with a 532 nm laser rated at 1.5 secchi depth, the CZMIL SuperNova is a dual frequency sensor with both a 532 nm and 1064 nm laser rated at 3.5 secchi depth.

Despite these differences, both sensors performed well in the relatively clear waters off the Aucilla River. **Figure 6** shows the depth response distribution for the ARI AOI derived from the VQ-880-G II and **Figure 7**, from the CZMIL SuperNova. It is apparent that the response was very comparable between the sensors, with

VEXCEL
IMAGING

DRAGON

Expand your perception

ULTRACAM

RIEGL inside

See why our brand-new UltraCam Dragon 4.1 is the perfect fit for your complex environment mapping projects.

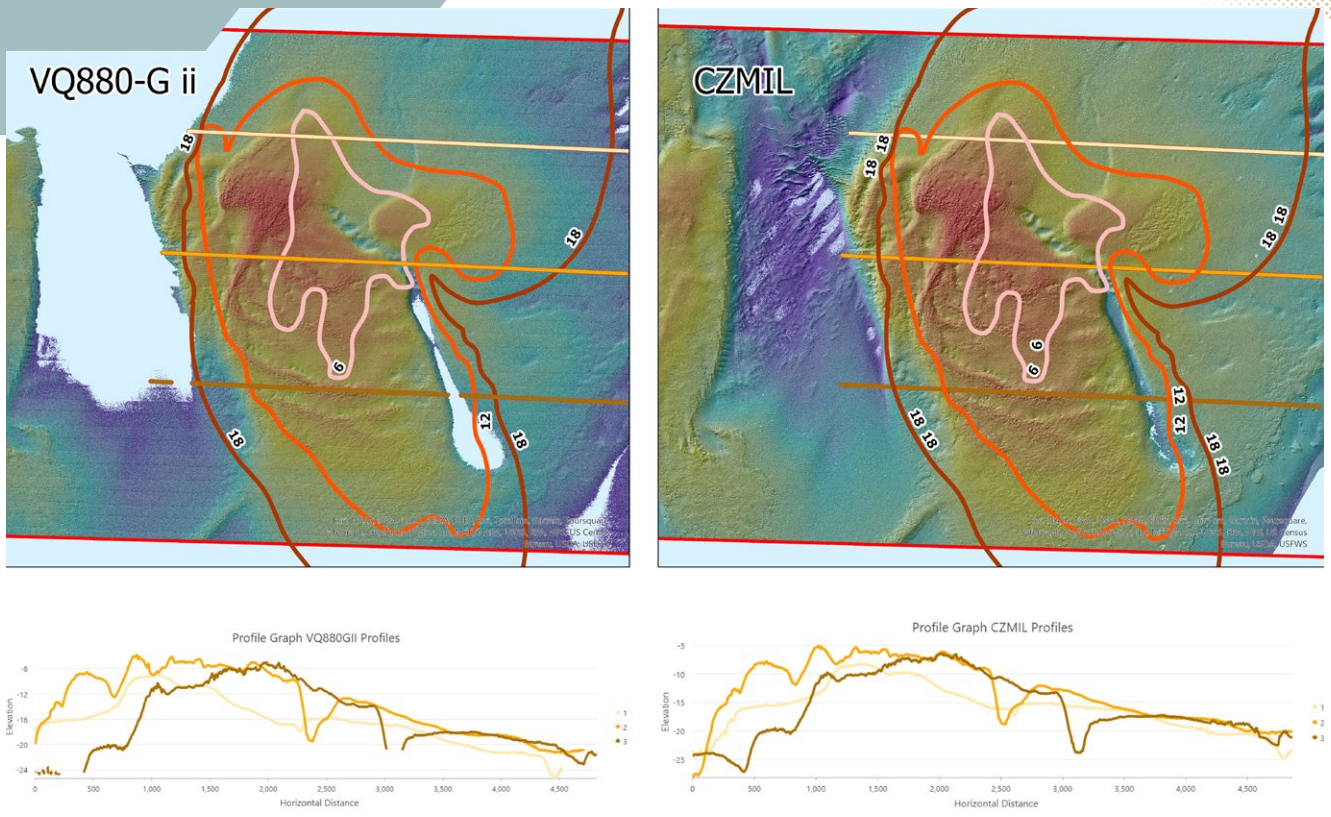

Figure 9: Topobathymetric lidar-derived DEMs with NOAA Nautical Chart 11450 contours and longitudinal profiles (top). Under each DEM is the color-coded plot of the profile elevations.

mean depths of -16.43' and -17.32' respectively. Similarly, the standard deviation in depth response was also comparable, 4.72' and 5.79' respectively. However, the range of depths recorded by the CZMIL SuperNova extended both higher (-1.94' vs -2.53') and lower (-34.21' vs. -29.1') into the water column than those recorded by the VQ-880-G II. The excess number of recordings for the CZMIL SuperNova resulted from the increased coverage in deeper water (see **Figure 8**).

DEM comparison

Bare-earth topobathymetric DEMs were constructed by NV5 and Dewberry from the Riegl VQ-880-G II and CZMIL SuperNova lidar data, respectively. Esri ArcGIS Pro v3.1 was used to extract the CZMIL SuperNova/NOAA DEM to the extents of the ARI AOI, and to project (bilinear interpolation) and scale the CZMIL SuperNova/NOAA DEM to the coordinate reference system of the ARI AOI DEM.

> "NOAA Nautical Chart 11450 mapping the Ochlockonee Shoal has remained unchanged since 1881 C&GS work. There was little congruence between [its] isobaths and either of the DEMs constructed from topobathymetric lidar."

Figure 8 shows the unprocessed bathymetric DEMs as a hillshaded (5X exaggeration) raster. There are noticeable differences in coverage between the two DEMs. While the ARI/VQ-880-G II DEM shows depths to -29.1', the NOAA/SuperNova DEM shows depths down to

-34.2'; a full five feet lower. This depth range results in several void areas in the ARI/VQ-880-G II DEM, particularly to the west of the shoal, and along the finger to the east of the shoal. The higher elevations (in red) on the Ochlockonee Shoal and the smaller shoal to the west are also slightly better defined in the NOAA/CZMIL SuperNova DEM.

Comparison between the two lidar sensors and NOAA Nautical Chart 11450 (2020)

As previously noted, the NOAA Nautical Chart 11450 mapping the Ochlockonee Shoal has remained unchanged since the 1881 C&GS work. We digitized the 6', 12' and 18' isobaths from Chart 11450 and present those contours over the topobathymetric lidar-derived DEMs (**Figure 9**, top). Then we constructed three longitudinal profiles through the shoal and plotted the elevations along the profiles (**Figure 9**, bottom) for each topobathymetric lidar-derived DEM.

In general, the profile elevations are very similar to each other and bear little resemblance to the contours from NOAA Nautical Chart 11450. The center profile, in orange, shows a very gradual, but steady, slope to the east and the southern profile, in dark orange, shows a very steep rise to the shoal area. Neither of the profiles shows close agreement to the NOAA Chart 11450 contours.

Summary

Both sensors, the RIEGL VQ-880-G II and the Teledyne Geospatial CZMIL SuperNova, performed very well in the near-shore waters off the Aucilla River in the Big Bend region of Florida. The CZMIL SuperNova achieved returns from water depths to over 34 feet while the VQ-880-G II achieved returns to a little over 29 feet of water. This difference results in void areas in the DEM derived from the VQ-880-G II data that were not void in the DEM from the CZMIL SuperNova data.

There was little congruence between NOAA Nautical Chart 11450 Ochlockonee Shoal isobaths and either of the DEMs constructed from topobathymetric lidar. While the topobathymetric lidar data was collected more than 140 years after the hydrographic survey that was used to produce the NOAA Nautical Chart, the utility of topobathymetric lidar data for updating bathymetric data in the area of the Ochlockonee Shoal, and most likely the entire area of NOAA Nautical Chart 11450, is clearly demonstrated.

Alvan "Al" Karlin, Ph.D., CMS-L, GISP is a senior geospatial scientist at Dewberry, formerly from the Southwest Florida Water Management District (SWFWMD), where he managed all the remote sensing and lidar-related projects in mapping and GIS. With Dewberry, he serves as a consultant on Florida-related lidar, topography, hydrology, and imagery projects, as well as general GIS-related projects. He has a PhD in computational theoretical genetics from Miami University in Ohio. He is vice president of ASPRS, a director of the ASPRS Florida Region, an ASPRS Certified Mapping Scientist-Lidar, and a GIS Certification Institute Professional.

George Cole, Ph.D., PSM, PLS is a professional land surveyor and engineer. His background includes service with the U.S. Coast and Geodetic Survey with a final rank of Lt. Commander, as the Chief of the Florida Department of Natural Resources Bureau of Surveying and Mapping, as an engineer with the Florida Department of Transportation, many years of private surveying and engineering practice, and as an adjunct professor at the University of Puerto Rico

References

Basillie, J.H. and J.F. Donaghue, 2011. Northern Gulf of Mexico sea-level history for the past 20,000 years. In Buster, N.A. and C.W. Holmes (eds.), *Gulf of Mexico: Origin, Water, and Biota. Volume 3: Geology*, Texas A&M Press, College Station, Texas, 446 pp, 53-72.

Cole, G.M., 2021. Mapping the Ochlockonee Shoal, *Monticello News*, November 24, 2021. https://ecbpublishing.com/mapping-the-ochlocknee-shoal-george-m-cole-aucilla-research-institute/.

Cole, G.M. and J.E. Ladson, 2020. The Aucilla in the Civil War, *Monticello News*, September 3, 2020. https://ecbpublishing.com/the-aucilla-in-the-civil-war/.

Holmes, C.W., 2011. Development of the northwestern Gulf of Mexico continental shelf and coastal zone as a result of the Late Pleistocene-Holocene sea-level rise. In Buster, N.A. and C.W. Holmes (eds.), *Gulf of Mexico: Origin, Water, and Biota. Volume 3: Geology*, Texas A&M Press, College Station, Texas, 446 pp, 195-208.

AIRBORNE LIDAR

A Tutorial for 2025

Part I: Lidar basics

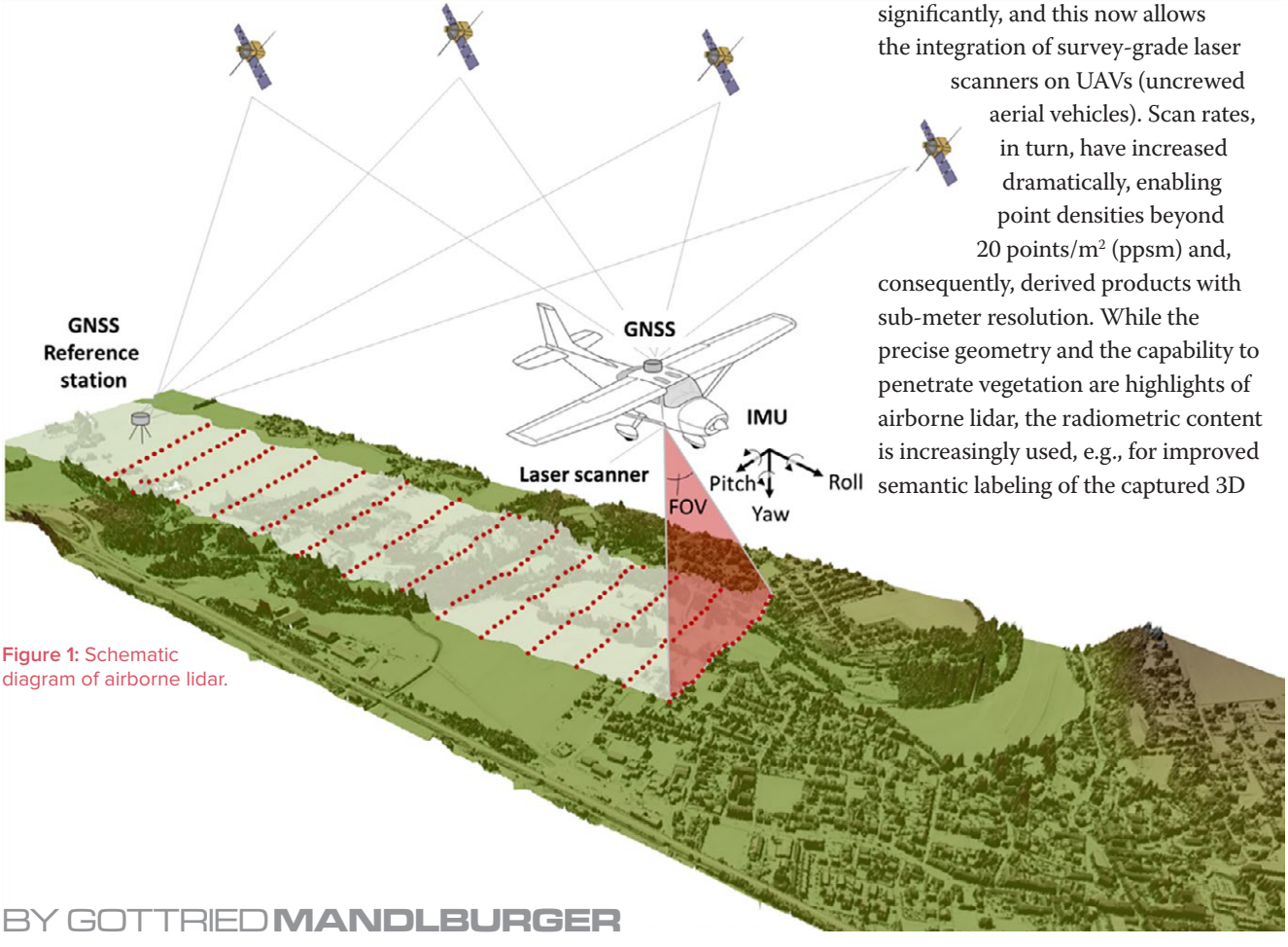

Figure 1: Schematic diagram of airborne lidar.

Since the beginning of the 21st century, airborne lidar (light detection and ranging) has entirely revolutionized topographic data acquisition. National mapping agencies around the globe have quickly adopted this active remote sensing technology and gradually changed their production workflows for the generation of national and transnational digital terrain models (DTMs). Over the last 25 years, enormous progress has been made in both sensor technology and data processing strategies. The weight and size of sensors has decreased significantly, and this now allows the integration of survey-grade laser scanners on UAVs (uncrewed aerial vehicles). Scan rates, in turn, have increased dramatically, enabling point densities beyond 20 points/m^2 (ppsm) and, consequently, derived products with sub-meter resolution. While the precise geometry and the capability to penetrate vegetation are highlights of airborne lidar, the radiometric content is increasingly used, e.g., for improved semantic labeling of the captured 3D

BY GOTTFRIED MANDLBURGER

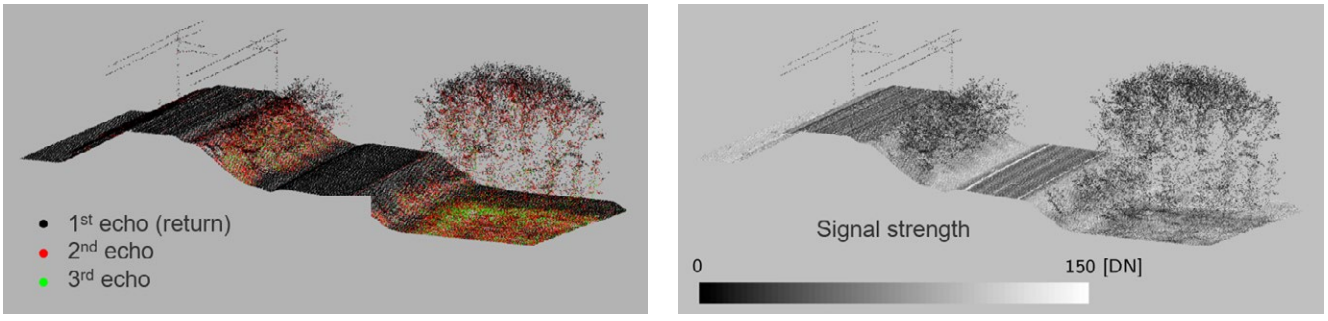

Figure 2: 3D airborne lidar point cloud: colored by echo number (left); colored by reflectance (right).

point cloud. The aim of this four-part tutorial is to revisit the principles of airborne lidar and to discuss current trends. While Part I covers the basics, Parts II-IV provide details about integrated sensor concepts, laser bathymetry and UAV-lidar.

The underlying concept

Airborne lidar is a kinematic 3D data acquisition method delivering 3D point clouds of the Earth's surface and objects thereon like buildings, infrastructure, and vegetation. The three main components are: (i) the laser scanner consisting of the lidar unit (ranging) and the beam deflection unit (scanning), (ii) a Global Navigation Satellite System (GNSS) for measuring the platform's position in a Cartesian, georeferenced coordinate system, and (iii) the Inertial Navigation System (INS) delivering the platform's attitude.

For the sensor system depicted in **Figure 1**, the laser beams are continuously sweeping in the lateral direction and, because of the forward motion of the platform, a swath of the terrain below the aircraft is captured. The distances between the sensor and targets on the ground are determined by measuring the roundtrip time of an outgoing laser pulse and the portion of the signal scattered back from the illuminated targets into the receiver's field of view (FoV). This is commonly referred to as the time-of-flight (ToF) measurement principle. To obtain 3D coordinates of an object in a georeferenced coordinate system (e.g., WGS84), the position and attitude of the platform and the scan angle need to be measured continuously in addition to the ranges. Thus, airborne lidar is a time-synchronized multi-sensor system, and the 3D points are calculated via direct georeferencing. For obtaining a positional accuracy of the flight path (trajectory) in the centimeter range, it is indispensable to use a GNSS base station located in the survey area. This could be either a permanent or virtual station of a GNSS service provider or a GNSS receiver installed on a tripod at a reference point with known coordinates.

Parameter	Unit	Value
Flying altitude	m above ground	500-4000
Scan Rate	kHz	100-6000
Laser beam divergence	mrad	0.1-1
Footprint diameter @ 1000 m	cm	10-100
Laser wavelength (topographic lidar)	nm	900-1550
Point density	points/m² (ppsm)	8-30
Vertical uncertainty	cm	1-10
Positional uncertainty	cm	5-25

Table 1: Specifications of modern airborne lidar sensors.

The ideal laser ray is infinitely small, but in practice the actual laser beams can be thought of as light cones with a narrow opening angle. The typical diameter of the illuminated spot on the ground (footprint) is in the cm- to dm-range depending on the flying altitude and the sensor's beam divergence. Representative specifications of state-of-the-art airborne lidar sensors are summarized in **Table 1**.

Due to the finite footprint, multiple objects along the laser line-of-sight are illuminated by a single pulse and ToF sensors can return multiple points for a single laser pulse. In addition, airborne lidar sensors typically deliver additional attributes for each detected laser point,

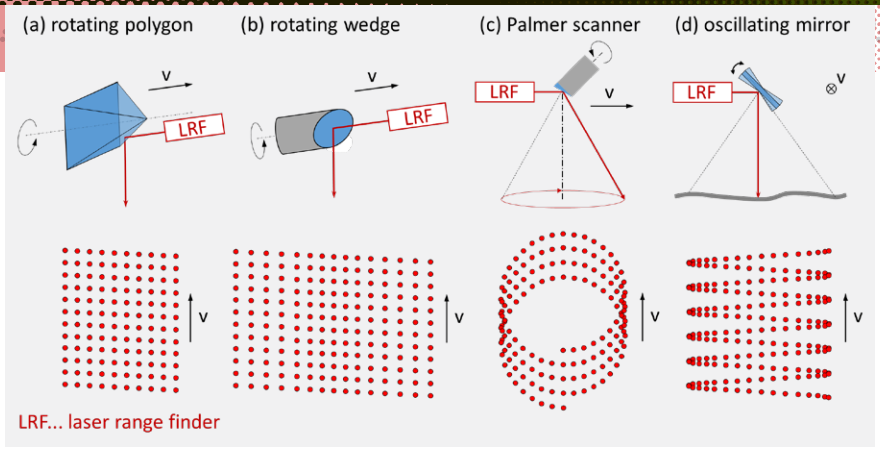

Figure 3: Laser beam deflection with rotating and oscillating mirrors.

such as signal strength (intensity) or reflectance (calibrated radiometry). An example is depicted in **Figure 2**, highlighting both the penetration capability of airborne lidar and its ability to capture radiometric information. The scene shown has complete ground point coverage with 1st echoes (black) in the open areas and 2nd and 3rd echoes (red, green respectively) in the overgrown parts (**Figure 2a**). **Figure 2b** shows the radiometric content where, for example, the road boundary lines stand out in white (i.e. with high reflectance).

Laser ranging

The core component of each laser scanning system is the ranging unit. The distance from the sensor to an object is generally estimated by measuring the round trip time of a short laser pulse (ToF). Given the speed of light c, the pulse emission time t_0, and the arrival time of the return pulse t_1, the sensor-to-target distance R can be calculated as:

$$R = \frac{(t_1 - t_0)}{2} c \qquad \text{EQ1}$$

The phase-shift method, which constitutes an alternative to the ToF approach, is specifically used in terrestrial laser scanning. In this case, a continuous laser signal is imprinted on to a carrier wave and the offset between the phases of the emitted and returned (modulated) signals is measured. The main advantage of the ToF principle is its inherent multi-target capability, i.e., multiple returns along the laser line of sight can be extracted from a single laser pulse (cf. **Figure 2a**). This is particularly useful for surveys in vegetated areas. The phase-shift technique, in contrast, only delivers a single return per pulse.

Scanning

In airborne lidar, sampling of the Earth's surface is carried out based on flight strips (cf. **Figure 1**). Areal coverage with 3D points requires (i) the forward motion of the aircraft and (ii) a beam deflection unit systematically steering the laser rays below or around the sensor. **Figure 3** shows typical beam deflection mechanisms and their resulting point patterns on the ground.

Rotating, multi-faced polygonal wheels create parallel scan lines on the ground approximately perpendicular to the flight path. By adjusting the rotation speed, flying velocity, and pulse repetition rate, a homogenous point distribution on the ground can be achieved within a ±30° FoV around the nadir. A scan wedge with a single mirror tilted by 45° allows for scanning the full vertical plane (360° panoramas). Palmer scanners use a tilted rotational axis of the mirror and produce a spiral scan pattern on the ground. Such a conical scanning yields a constant incidence angle of the laser beam with respect to a horizontal ground plane, which is specifically useful for laser bathymetry to keep the angle between laser beam and water surface constant. Palmer scanners are also used in topographic laser scanning to enable views under bridges and to capture terrain and buildings from different angles. The point density is less homogeneous, however, as significantly higher densities are achieved at the strip boundary than in the center of the strip. A further disadvantage is the lack of nadir views. Finally, oscillating mirrors swing repeatedly between two positions. This scanning mechanism also leads to a higher point density at the edge of the strip due to the necessary deceleration and re-acceleration of the mirror in the opposite direction.

Signal detection

In conventional ToF laser ranging, the return signal of a highly collimated laser pulse is received by a single detector. For the conversion of the optical power into digital radiometric information, a two-stage procedure is employed. First, an avalanche photo diode (APD) converts the received laser radiation into an analog signal, and subsequently an analog-to-digital converter (ADC) generates the final measurement in digital form. APDs used for airborne laser scanning operate in linear-mode, i.e. within the dynamic range of the APD the optical power and the analog output are linearly related. Such APDs deliver measures of the received signal strength and provide object reflectance and/or material properties of the illuminated

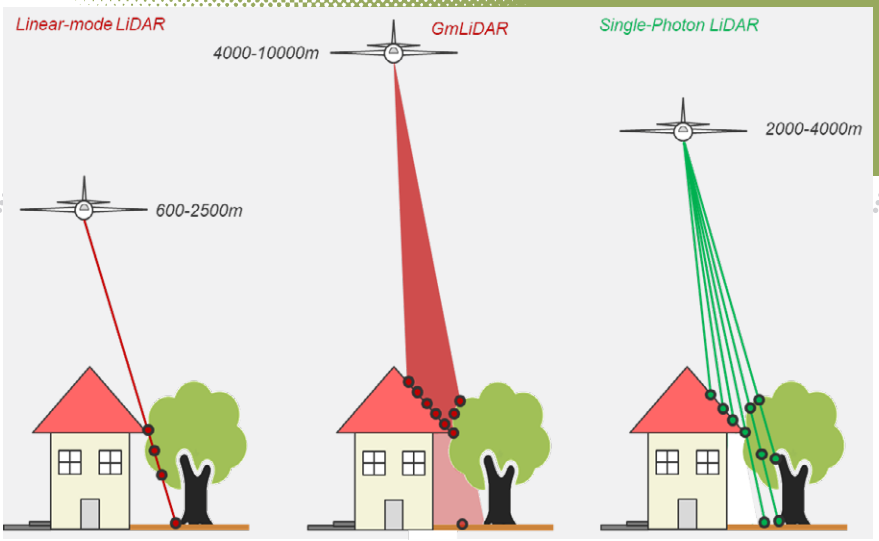

Figure 4: Schematic diagram of the three lidar modes.

objects via radiometric calibration.

The actual range detection is implemented either by hardware components of the laser scanner (discrete echo systems) or by high-frequency discretization of the entire backscattered echo waveform (full waveform). In the latter case, the captured waveforms are either processed online by the firmware of the sensor or stored for detailed analysis in post-processing. Storing the full waveforms enables the application of sophisticated signal post-processing, e.g., Gaussian decomposition offers advantages with respect to ranging precision, target separability, and object characterization (amplitude, echo width, reflectance, etc.). Nevertheless, at least several hundred photons are required for a reliable detection of a single object.

A different approach is Geiger-mode lidar (Gmlidar), where a divergent laser pulse is emitted, resulting in a large laser footprint on the ground. The return signal is captured by a Geiger-mode avalanche photo diode (GmAPD) array, i.e., a matrix of single-photon-sensitive receiver elements. The APD of each single matrix element is operated in Geiger-mode, whereby an additional bias above the break-through voltage brings the detector into a state where the arrival of a single or a few photons is sufficient to trigger the avalanche effect, leading to an abrupt rise of voltage at the receiver's output. The break-through event of the photodiode triggers the stop impulse for the range estimation via a time-to-digital convert (TDC). After a break-through event, the respective cell is inactive for a period, so only a single echo can be measured per APD cell from the same laser pulse.

In contrast, the technology referred to as single-photon lidar (SPL) utilizes a short laser pulse, which is split into a grid of 10x10 sub-beams (beamlets) by a diffractive optical element (DOE). The 100 beamlets are highly collimated, thus their footprints on the ground do not overlap. For each beamlet, the backscattered signal is received by an individual detector, which is aligned to the laser beam direction. Each detector, in turn, consists of a matrix of several hundred single-photon-sensitive cells, each operating in Geiger-mode. Possible implementations of this technique include micro channel plate photomultiplier tubes or silicon photomultipliers. Within a restricted dynamic range, each beamlet detector acts like an APD operated in linear-mode, which enables moderate multi-target capabilities. For both SPL and Gmlidar, the receiver's single photon sensitivity enables higher flying altitudes and consequently a potentially higher area performance. This is especially relevant for nationwide topographic mapping. A schematic diagram illustrating the three different options (linear-mode lidar, Gmlidar, SPL) is sketched in **Figure 4**.

Geometric sensor model

As stated above, airborne lidar is a kinematic measurement process based on a tightly synchronized multi-sensor system consisting of a GNSS receiver, an INS, and the laser scanner itself. The computation of georeferenced 3D points is called direct georeferencing and is illustrated in **Figure 5**.

The standard airborne lidar data processing pipeline starts with

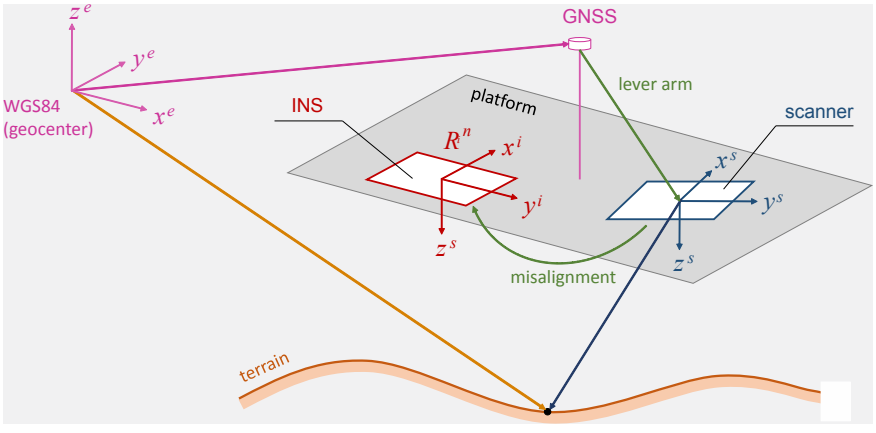

Figure 5: Schematic diagram of the geometric airborne lidar sensor model.

calculating the platform's trajectory using Kalman filtering of the GNSS and INS observations. This results in a so-called smoothed best estimate of trajectory (SBET), constituting the absolute 3D positions (X, Y, Z) of the measurement platform in a geocentric, Cartesian (Earth-centered, Earth-fixed: ECEF) coordinate frame as well as the attitude of the measurement platform with respect to the local horizon (navigation angles: roll, pitch, yaw). In the next step, the trajectory data are combined with the time-stamped laser scanner measurements. Here, the manufacturers typically compensate small systematic instrument effects of the ranging and scanning unit based on laboratory calibration and directly provide corrected 3D coordinates of the detected objects (i.e. laser echoes) in the sensor coordinate system. These constitute the basis for the calculation of 3D object coordinates in an ECEF coordinate system according to **Equation 2**:

$$x^e(t) = g^e(t) + R_n^e(t)R_i^n(t)(a^i + R_s^i x^s(t)) \quad \text{EQ2}$$

The transformation chain in **Equation 2** transforms between the following coordinate systems (CS), each denoted by a specific index and highlighted by a specific color in **Figure 5**.

- s/blue: scanner CS
- i/red: INS CS
- n/no color: navigation or platform CS (i.e. local horizon CS: north/east/down)
- e/magenta: ECEF (Earth-centered, Earth-fixed) CS

Reading **Equation 2** from right to left, $x^s(x^s, y^s, z^s)$, the 3D point in the local scanner CS, is rotated by the boresight angles into the INS system (R_s^i) and shifted by the lever arm (a^i). The lever arm is the offset vector between the phase center of the GNSS antenna and the origin of scanner system, and the boresight angles denote the small angular differences (Δroll, Δpitch, Δyaw) between the reference planes of the scanner and the INS, respectively (cf. green elements in **Figure 5**). R_i^n transforms the resulting vector from the INS CS to the navigation CS (local horizon CS) based on the roll, pitch, and yaw angles measured by the INS, and R_n^e rotates to the Cartesian ECEF system. The latter rotation depends on the geographical position (latitude/longitude) of the INS origin. The 3D coordinates of the laser point $x^e(t)$ are finally obtained by adding the ECEF coordinates of the GNSS antenna (g^e).

The total positional and vertical uncertainty (TPU/TVU) of the 3D laser points depend on the accuracy of both the laser scanner and the trajectory, as well as on the synchronization of all sensor components (GNSS, INS, scanner). Modern laser scanners provide a ranging accuracy of 1-3 cm. Integrating the GNSS observation of both the base station and the lidar sensor system in post-processing yields an accuracy of 3-5 cm. Typical accuracies for INS employed for airborne lidar are 0.0025° for roll/pitch and 0.005° for the heading (yaw) angle. Overall, state-of-the-art airborne lidar sensors deliver sub-dm 3D coordinate accuracy.

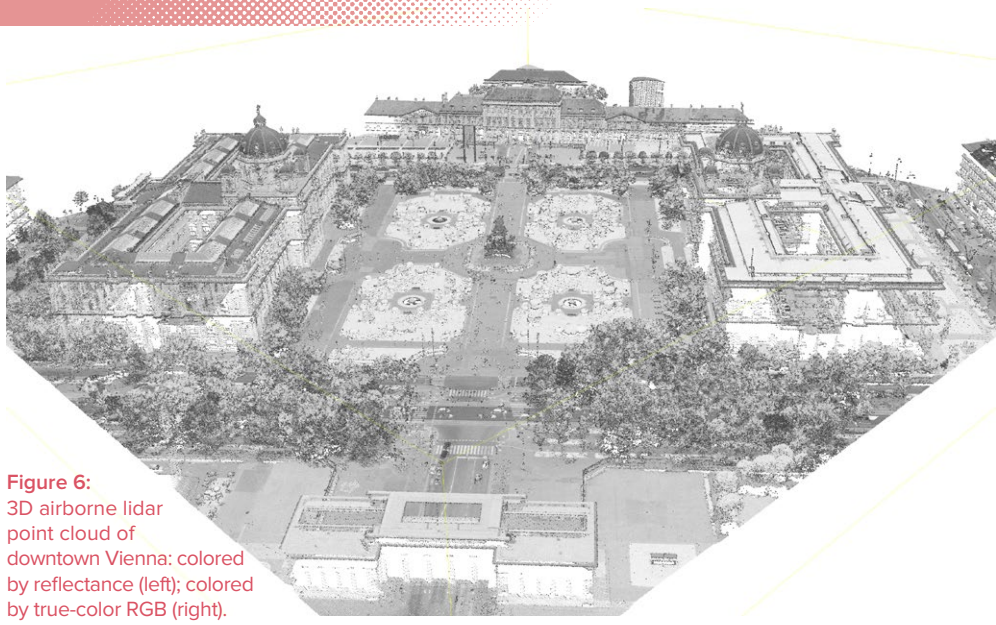

Figure 6: 3D airborne lidar point cloud of downtown Vienna: colored by reflectance (left); colored by true-color RGB (right).

Radiometric sensor model

Information about the radiometric properties of illuminated objects is of high importance, e.g., for semantic point cloud labelling and for many follow-up applications. The laser-radar equation describes the fundamental relationship between the transmitted and the received optical power:

$$P_R = \frac{P_T D^2}{4\pi(\gamma R)^2} \sigma \eta_{ATM} \eta_{SYS} + P_{BK} \quad \text{EQ3}$$

The received power P_R depends on the transmitted power P_T, the measurement range R, the laser beam divergence γ, the size of the receiver aperture D , the

backscattering cross-section σ, as well as factors related to system losses η_{SYS} and η_{ATM}. P_{BK}, finally, indicates solar background radiation that deteriorates the signal-to-noise ratio.

The backscattering cross-section σ incorporates all target properties and can be separated into the illuminated target area (A), the object's reflectance (ρ) , and the backscattering solid angle (Ω).

$$\sigma = \frac{4\pi}{\Omega} A\,\rho \qquad \text{EQ4}$$

Small values of Ω relate to specular reflection (e.g., on water or glass surfaces). In turn, most of the natural targets (soil, grass, trees, etc.) as well as sealed surfaces (asphalt, concrete) are diffuse scatterers. For ideal diffusely reflecting targets (Ω = 180°), Lambert's cosine law is applicable. The cross-section further depends on the illuminated area A, which is a function of the measurement range R, the beam opening angle γ, and the incidence angle between the laser beam and the normal direction of the illuminated surface. While the most generic formulation of the laser-radar equation reveals a decay of the received power with R^4, the signal loss for targets that are fully covered by a single laser footprint is limited to R^2 as written in **Equation 3**. Typical examples of such extended targets include points on open terrain, roads or building roofs.

In summary, the received total power (intensity) measured by airborne lidar sensors strongly depends on the measurement range and other factors. To make the radiometric content comparable among different flight strips and, beyond that, among different flight missions, homogenization of the measured raw intensities is inevitable. Simple correction strategies account for the dominating range effect to correct the received signal strength measurements, and more rigorous approaches apply radiometric calibration based on external radiometric reference measurements to obtain object properties such as backscattering cross-section or object reflectance. **Figure 6** shows an example from an airborne lidar campaign in Vienna. The scene depicts the square of empress Maria-Theresia (Maria-Theresien-Platz) between the Museums of Fine Arts and Natural History. The 3D point cloud is greyscale-colored by calibrated reflectance and by true-color RGB. The latter requires the integration of a laser scanner and a camera. Such integrated sensor systems are the main topic of Part II of this tutorial, which will appear in the next issue of *LIDAR Magazine*.

Dr. Gottfried Mandlburger studied geodesy at TU Wien, where he also received his PhD in 2006 and habilitated in photogrammetry with a thesis on "Bathymetry from active and passive photogrammetry" in 2021. In April 2024 he was appointed University Professor for Optical Bathymetry at TU Wien.

His main research areas are airborne topographic and bathymetric lidar from crewed and uncrewed platforms, multimedia photogrammetry, bathymetry from multispectral images, and scientific software development. Gottfried Mandlburger is chair of the lidar working group of Deutsche Gesellschaft für Photogrammetrie und Fernerkundung, Geoinformation e.V. (DGPF) and Austria's scientific delegate in EuroSDR. He received best paper awards from ISPRS and ASPRS for publications on bathymetry from active and passive photogrammetry.

Further reading

Mallet, C. and F. Bretar, 2009. Full-waveform topographic lidar: State-of-the-art, *ISPRS Journal of Photogrammetry and Remote Sensing*, 64(1): 1–16.

Shan, J. and C.K. Toth, 2018. *Topographic Laser Ranging and Scanning: Principles and Processing, Second Edition*, Taylor & Francis, Boca Raton, Florida, 637 pp.

Vosselman, G. and Maas, H.-G. (eds.), 2010. *Airborne and Terrestrial Laser Scanning*, Whittles Publishing, Dunbeath, Caithness, Scotland, 336 pp.

Wagner, W., 2010. Radiometric calibration of small-footprint full-waveform airborne laser scanner measurements: Basic physical concepts, *ISPRS Journal of Photogrammetry and Remote Sensing*, 65(6): 505–513.

Finding Connecticut's Historic Buildings In High-Density Lidar Point Clouds

Today's point densities and processing tools facilitate new applications

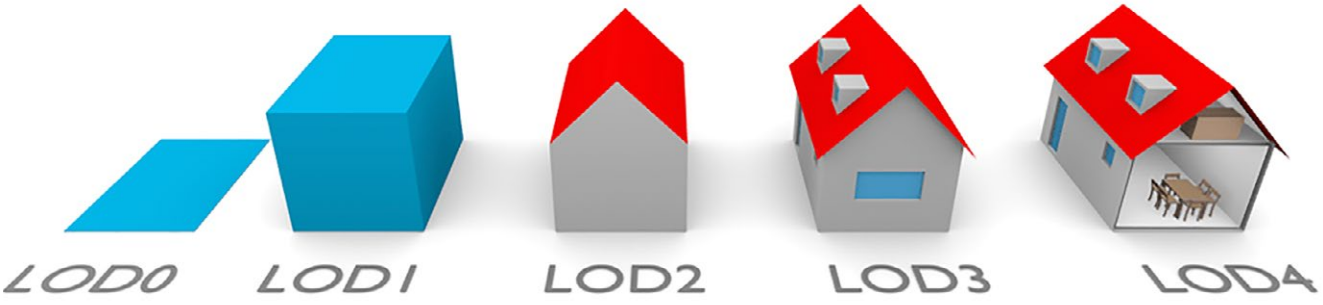

Figure 1: Increasing Levels of Detail (LOD) for 3D buildings from building footprints (LOD0) through photo-realistic modeled buildings (LOD4).

Most familiar lidar applications, such as terrain modeling, land development, and hydrology, focus on the bare-earth model, a digital terrain model (DTM), which is constructed using only the "ground" points from the lidar point cloud. Recently, however, forestry, archaeological, and digital-twin applications moved the focus for lidar applications from the bare-earth model toward enhanced uses of other classes of lidar returns in the point cloud. New and emerging applications, along with the higher pulse density achieved by today's lidar sensors, have opened new avenues for lidar applications.

Aerial lidar has rapidly evolved from 1–2 pulses per square meter (ppsm) in the early 2000s, to 8–24 ppsm and even higher from uncrewed aerial vehicles. These high-density point clouds have been used to reveal anthropogenic features, sometimes entire cities (Khalil, 2023, 2024) that have been hidden from conventional aerial photogrammetry by dense vegetation. As pulse densities have increased and lidar sensors mounted on uncrewed aerial vehicles have become more common, detailed forestry and corridor transmission-line and transportation applications have also emerged. Most recently, high-density lidar and 3D modeling techniques have been merged to form the basis for constructing digital twins of entire US counties (Rich, 2023). As a result of these technologies coalescing and becoming affordable, municipalities have been eager to construct digital

BY AL **KARLIN** AND ANDREW **PETERS**

Figure 2: Typical issues requiring manual editing from automated building extraction. From left to right: "donut" holes interior to building outlines; multi-sided attached buildings; and parked semi-trailers.

representations of buildings to assist in emergency management, planning, and historic preservation (Marcoux and Leifeste, 2022).

In 2023, Dewberry, an Esri Gold Partner, was tasked by the State of Connecticut to conduct a high-density, high-precision lidar survey of the state. The data, collected at 20 ppsm, is intended to serve multiple purposes, for example as a base layer for the Connecticut Cultural Resources Information System (ConnCris[1]). This on-line viewer is maintained in conjunction with the Connecticut State Historic Preservation Office (SHPO). To meet these needs, along with the bare-earth model and classified lidar point cloud, Dewberry's deliverables include 3D building models (**Figure 1**).

3D building workflow

Dewberry evaluated the Level of Detail (**Figure 1**) required to meet the needs of SHPO. Following discussions with SHPO, Dewberry determined that LOD2 would meet both the economic and display requirements for the ConnCris viewer. Having focused on LOD2, Dewberry employed the Esri building extraction tools in the 3D Analyst Extension for the initial 3D building construction, using the "standard" workflow of (1) generating a bare-earth DEM, (2) extracting building footprints (LOD0), (3) classifying noise and building returns, (4) some manual clean-up of building footprints, and (5) applying the LAS Building Multipatch tool in ArcGIS Pro/3D Analyst to produce the LOD2 3D buildings.

Typical issues encountered with this workflow that required manual intervention in the automated Esri "standard" 3D building extraction workflow included the expected "donut" holes interior to polygons (**Figure 2**, left), connected multi-sided buildings (**Figure 2**, center) and parked trailers (**Figure 2**, right). These issues were resolved by manual intervention.

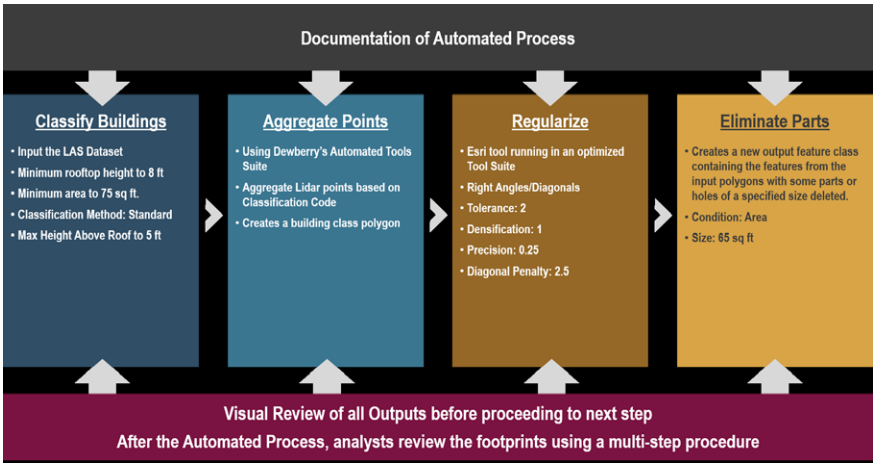

Figure 3: Dewberry's modified workflow incorporating the Esri 3D Analyst tools and manual editing to produce 3D buildings to the ConnCriss specifications.

1 https://conncris.ct.gov/

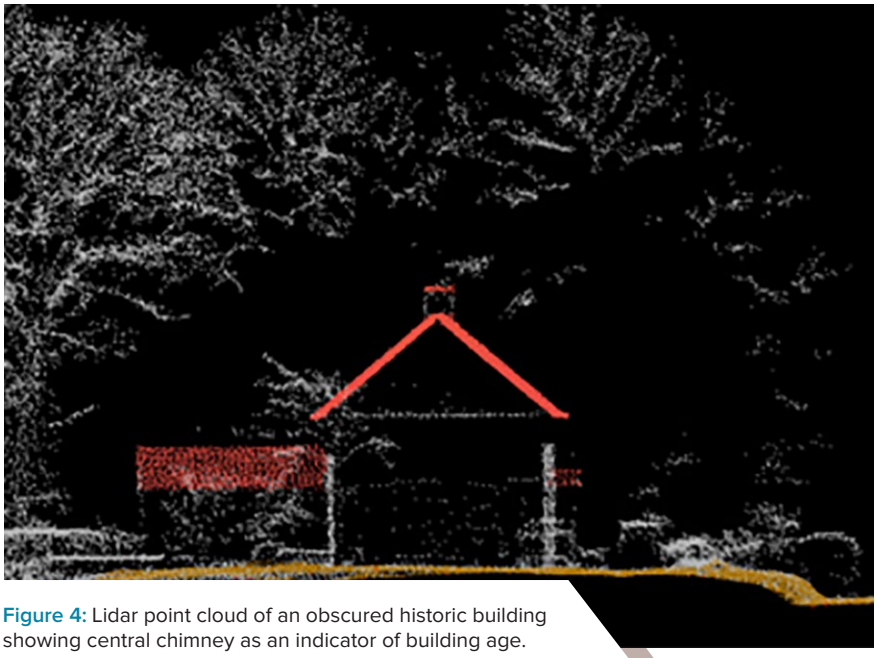

Figure 4: Lidar point cloud of an obscured historic building showing central chimney as an indicator of building age.

> Using [a custom] workflow, Dewberry identified over 1.2 million buildings. Those houses with central chimneys were identified as historic structures.

To facilitate and optimize the building extraction process, Dewberry integrated the standard Esri tools into custom toolsets, then constructed a detailed workflow, including the manual quality assurance (QA) steps (**Figure 3**). This workflow produced 3D buildings with a minimum size of 75 square feet and a roof height of more than 8 feet, to meet the ConnCris criteria. Using this modified workflow, Dewberry identified over 1.2 million buildings.

Historic buildings

The history of Connecticut predates the Revolutionary War (1775-83) and this is reflected in the cultural artifacts in the State. SHPO maintains the database for historic buildings built prior to 1880. Using the modified Esri 3D building workflow, Dewberry was able to identify the chimney position in the 3D buildings. Using this as the discriminating feature, those houses with central chimneys (**Figure 4**) were identified as historic structures. Several historic structures were obscured from photogrammetric detection under dense vegetation, but discoverable by lidar.

Alvan "Al" Karlin, Ph.D., CMS-L, GISP is a senior geospatial scientist at Dewberry, formerly from the Southwest Florida Water Management District (SWFWMD), where he managed lidar-related projects and Geographic Watershed Information System/Arc Hydro database development in cooperation with the Watershed Management Program. With Dewberry, he serves as a consultant on hydrology, topography, and imagery projects. He is currently vice president of ASPRS. In his spare time, he enjoys chasing after salamanders, frogs, lizards, and snakes, as well as growing tomatoes in his garden.

Andrew Peters, GISP is senior associate, assistant department manager at Dewberry. He has over 15 years of experience in managing and producing more than 30 large scale GIS projects for federal and state clients in 25 states. Andrew regularly blogs on elevation- and lidar-related issues. In addition to his work with GIS asset management, Andrew specializes in using GIS to assess data accuracy by comparing raw lidar data with ground survey data, generating bare-earth models, and developing GIS methods for contour-line creation, flood analysis, and other terrain studies.

References

Khalil, J. 2023. Lidar reveals a hidden Mayan city. *GPS World*, August 8, 2023. (https://www.gpsworld.com/lidar-reveals-a-hidden-mayan-city/).

Khalil, J. 2024. Lidar reveals lost cities in the Amazon. *GPS World*, January 22, 2024. (https://www.gpsworld.com/lidar-reveals-lost-cities-in-the-amazon/).

Marcoux, J. and A. Leifeste, 2022. Impact of digital technologies on historic preservation research at multiple scales. *Technology\Architecture + Design*, 6(1): 22–31. https://doi.org/10.1080/24751448.2022.2040299.

Rich, S. 2023. Digital twin boosts growth, sustainability planning in Maryland county. Esri Blog. https://www.esri.com/about/newsroom/blog/maryland-county-planning-digital-twin/.

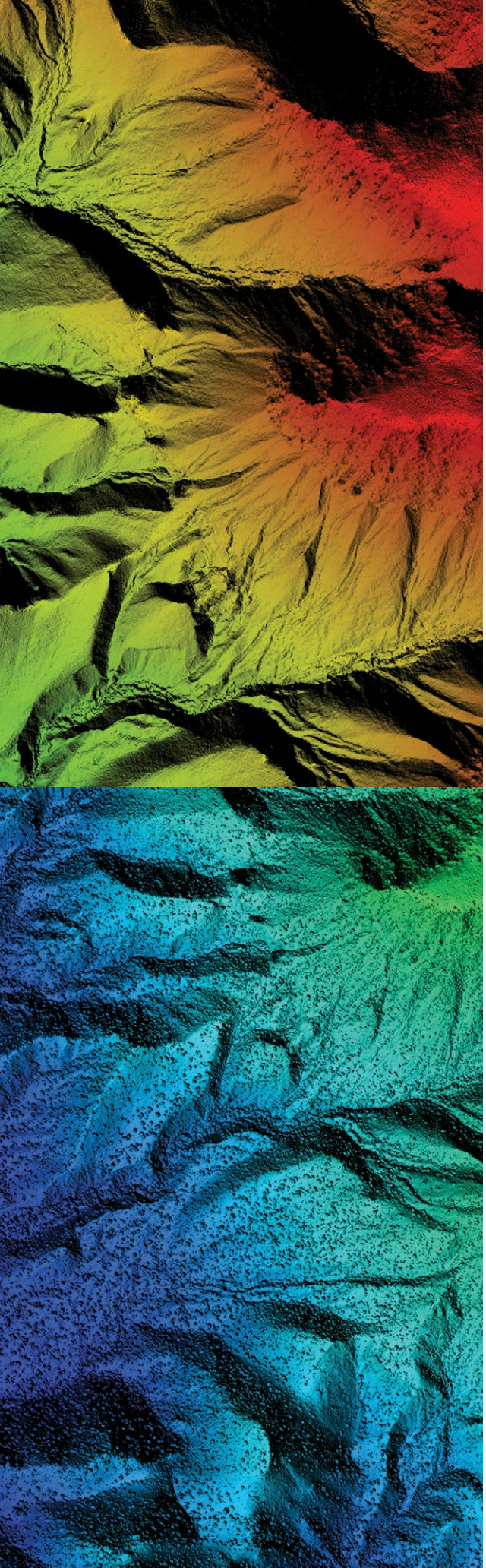

Your Strategic Geospatial Resource

- Classified lidar point cloud
- Hydro-flattening breaklines
- Digital Elevation Models
- Digital Surface Models
- Intensity images
- Hillshades
- Contours
- Elevation-Derived Hydrography (EDH)

Full Service Geospatial Services:

- Lidar Acquisition and Processing
- Digital Orthoimagery Acquisition and Processing
- Digital Topographic and Planimetric Mapping

Energy • Government • Engineering • Forestry

SURDEX CORPORATION

520 Spirit of St. Louis Blvd. • Chesterfield, MO 63005
636-368-4400 • surdex.com

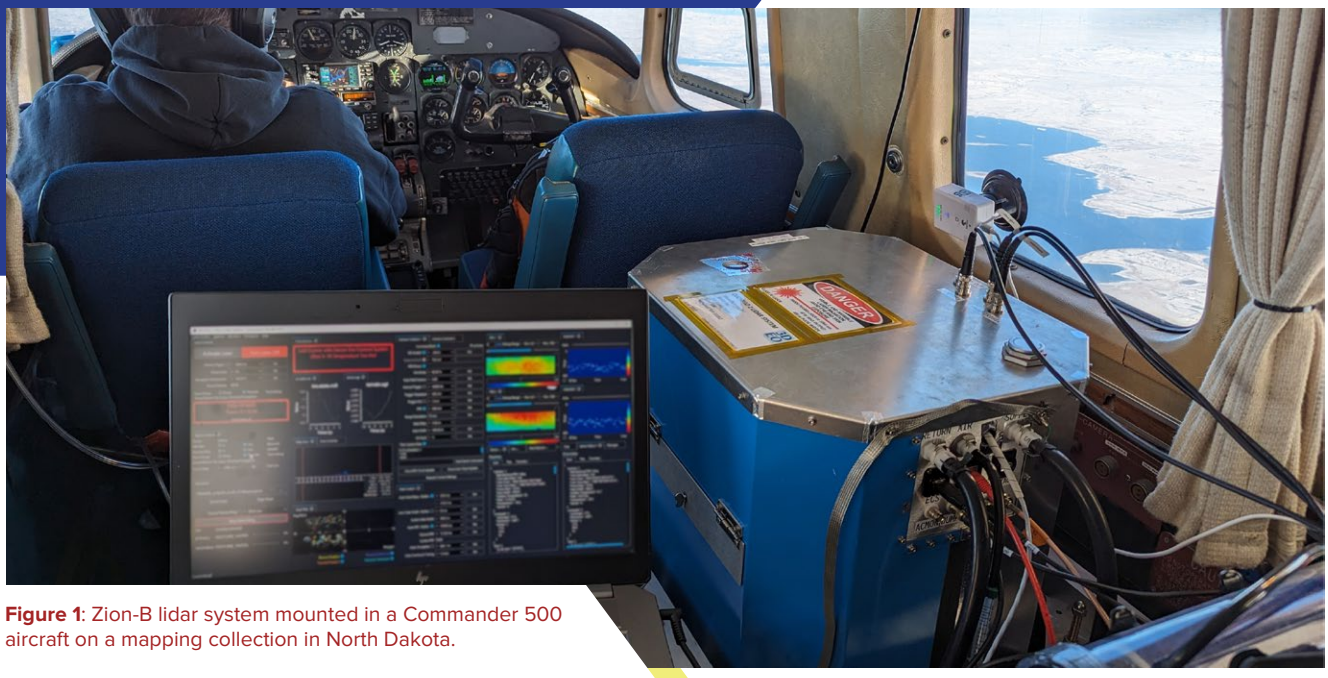

Figure 1: Zion-B lidar system mounted in a Commander 500 aircraft on a mapping collection in North Dakota.

Next-Generation Geiger-Mode Lidar Systems

3DEO advancing Geiger-mode lidar technology

Geiger-mode (GM) lidar has been operationally proven by the US military since 2010[1] and is seeing renewed interest in the commercial geospatial world. 3DEO, a spin-out from MIT Lincoln Laboratory, is providing advanced GM lidar systems to the commercial market. This includes sensor hardware and a suite of processing software that enables lidar operators to execute complete projects. GM lidar sensors are powerful tools for fast and efficient collection of highly detailed 3D point clouds for applications such as forestry, wildfire modeling, urban mapping, wide-area mapping, and disaster response.

The next-generation systems from 3DEO include the core GM lidar technology advantages of fast measurement

BY KIMBERLY S. **REICHEL-VISCHI** AND DALE G. **FRIED**

rates and exquisite sensitivity. They also embody significant advances over previous generations. A primary innovation is 3DEO's patent-pending agile geo-referenced scanning[2], which directs the full capability of the lidar into only specific areas of interest, such as a narrow winding corridor or campus, thus facilitating high diversity of collection geometries to mitigate shadowing. In addition, streamlined data processing workflows enable raw data from many different scans to be aggregated so that weak signals from significantly occluded surfaces can be turned into deliverable data products with high information utility. These innovations allow lidar operators to collect point clouds with the data densities commonly associated with UAV-lidar collections, but at a scale associated with larger aircraft. This large-scale, high-density data is a critical input for numerous applications.

The name "Geiger-mode" refers to the physical process by which the lidar detects the faint light pulses received by the lidar from the ground[3]. As each individual photon is received, an electrical pulse is detected and time-stamped, analogous to the clicks of a Geiger-counter detecting radioactivity. The "clicks" are processed into point clouds using the time of flight of the laser pulse. What is different from the more common "linear mode" lidar is the remarkable sensitivity. A point in the product point cloud is typically established using only 5–10 "clicks" of the GM photodetector, arising from 15–30 photons received by the lidar. In contrast, a typical linear-mode system needs a minimum of approximately 300 received photons to reliably differentiate a real surface from the noise in the system. Because of this 10–20x lower light requirement, GM lidar systems can collect data at high rates from higher altitudes, simplifying operations in rugged terrain and collecting wider swaths on the ground. GM lidars normally use an array of these sensitive photodetectors, all operating in parallel on every laser pulse; array sizes range from 32x32 to 128x256. More advanced GM lidars utilize multiple arrays, enabling area collection rates of, for example, 700 km^2 per hour at a point density of 50 points per square meter from an altitude of 10,000 ft (3000 m) 3DEO GM lidar sensors yield millions of interrogations per second, with a range resolution of 15–20 cm, and an angular resolution of 76 microradians, which at 3000 m (9800 ft) yields about 23 cm horizontal resolution. **Figure 1** shows 3DEO's Zion-B lidar system in operational use.

Essential to making these high point densities useful is collecting the point clouds from many different viewpoints to overcome the common shortcoming of shadowing and occlusions in lidar products. 3DEO has developed an agile geo-referenced scanning method[4] that provides the flexibility required to achieve high angular diversity, which is crucial in highly foliated scenes to "poke through" the foliage to the ground layer[5]. The combined laser and camera optical paths may be scanned anywhere in the 40° x 40° field of regard of the system. In a mapping style collection, the area is partitioned into multiple swaths with sufficient overlap. Each swath is broken up into polygons of several hundred meters size, and each polygon is scanned multiple times over the course of the flight path, resulting in several total looks per polygon. By engineering the polygons appropriately, the amount of angular diversity per pass can be matched to the needs of the project. For

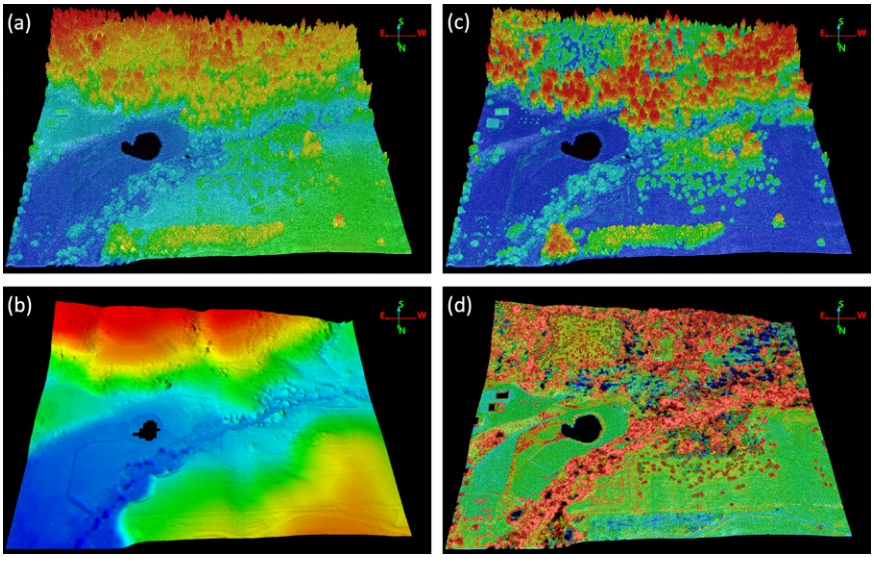

Figure 2: Sample mapping collection area of about 800 x 800 m in North Idaho, obtained with 3DEO's Zion-A sensor: (a) colored by elevation, range 775–833 m; (b) DTM generated by SHR3D[6], colored by elevation, range 775–808 m; (c) colored by height above ground (HAG), range 0–30 m; (d) cropped by HAG to 0–2 m, and recolored to highlight trails and other features in the human activity layer.

foliage penetration and urban mapping, typically high angular diversity is chosen, whereas for wide-area mapping of unforested scenes only a single scan of each polygon is needed.

To make use of the high angular diversity from many views, 3DEO has developed a processing workflow and algorithms to coalesce all the information into one representation of the scene. The raw sensor data is extracted to create a raw 3D point cloud for each individual scan. The scans are aligned, combined and then processed together in order to find surfaces whose lidar echoes were too weak to detect from any single scan. The level of detail in the scenes of the aggregated point cloud can be compared to point densities obtained with traditional UAV-lidar but obtained at a much higher area collection rate. From the aggregated point clouds, standard derived products may be obtained such as bare earth digital terrain models (DTMs), digital surface models (DSMs), and height above ground (HAG).

To show how all these unique characteristics of 3DEO's GM lidar sensors combine together, we present a practical example of a site in North Idaho, which was collected from 5000 ft (1500 m) above ground level (AGL) at a rate of 45–50 km^2 per hour per pass using our first-generation mapping system, Zion-A. The mapping was designed to probe everywhere on the ground from two flight passes offset from each other to illuminate two opposite sides of objects. The effective area collection rate was 27 km^2 per hour. The area collected was about 68 km^2, and each polygon was about 400 m x 400 m. Each polygon was scanned approximately eight times over the course of the two passes. **Figure 2** shows the same sample area four different ways. The area is comprised of four abutting polygons, covering an area of about 800 x 800 m. The four different panels show different cropping and coloring schemes to indicate data utility. **Figure 3** shows a transect through a portion of the area with high foliage. A ground layer is clearly visible as well as the stems of the trees. This level of detail and simultaneous fast acquisition rate are made possible by GM technology:

3DEO
Fast, Efficient 3D Imaging

Dale Fried founded 3DEO, Inc.* in 2014 after developing advanced GM lidar systems and concepts for the US Government at MIT Lincoln Laboratory. It became clear that features of GM lidar that were compelling for defense and security applications were also attractive in the commercial geospatial world: high data collection rate, high sensitivity to weak returns, flexible software-based signal extraction techniques, and scanning techniques enabled by camera-based receivers.

3DEO has grown organically without external investments through engineering consulting and data-collection projects, and now offers complete GM lidar systems for sale and lease. The complete systems include software tools for mission planning, airborne GM sensor hardware, and 3DEO-developed software for extracting the raw data into 3D point clouds, all developed by 3DEO. To ensure that sensor operators have confidence in the final data products they deliver to their customers, 3DEO provides a complete software suite for processing, allowing them to control the workflow and establish predictable product quality.

3DEO is privately held, with employees holding the great majority of the equity rights. The team is dedicated to building "the kind of company we want to work at". 3DEO takes personal interest in the success of its clients and customers, helping them understand where and how the technology may be useful in their projects. Customized solutions are often crafted to meet unique challenges. 3DEO is headquartered in Norwood, Massachusetts, near Boston's academic and high-technology communities. The Norwood offices and laboratory are located at the Norwood Municipal Airport (KOWD). 3DEO's second office is in Orem, Utah, near local universities and the incredible outdoor recreational opportunities of the mountain west. 3DEO's third office is in Frankfort, Indiana, the middle of America's heartland.

3DEO staff includes: founder Dale Fried, who serves as CEO; Brandon Call (joined 2015), director of software engineering; and Christopher Reichert (joined 2017), director of lidar operations. Chris, Brandon, and Dale worked together at MIT Lincoln Laboratory on GM lidar programs for DoD intelligence, surveillance, and reconnaissance applications such as wide-area mapping and foliage penetration. 3DEO's team has grown to 15 technical and professional staff, including a dozen engineers and physicists.

* www.3deolidar.com

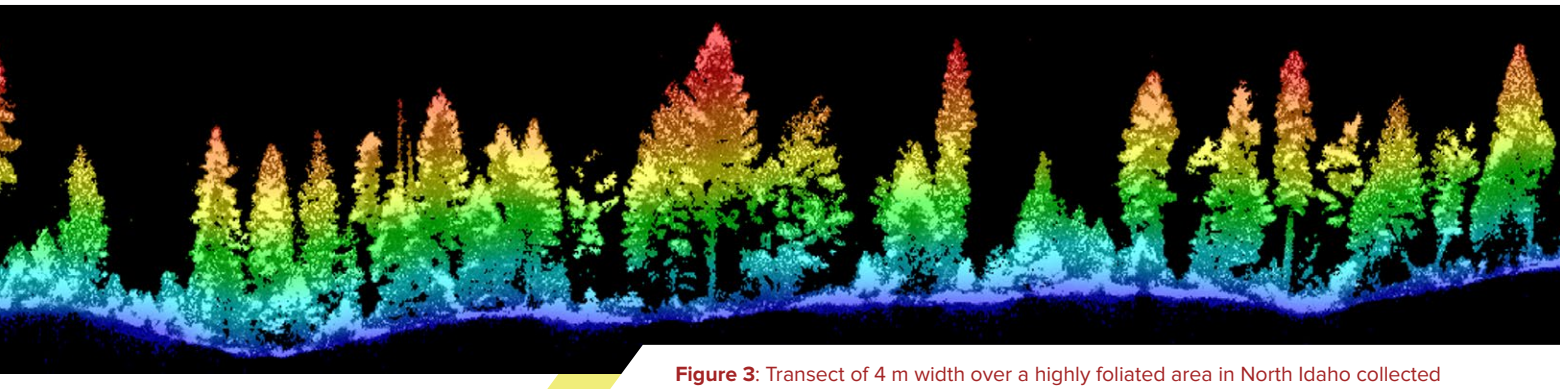

Figure 3: Transect of 4 m width over a highly foliated area in North Idaho collected by 3DEO's Zion-A sensor. Colored by height above ground, range 0–30 m.

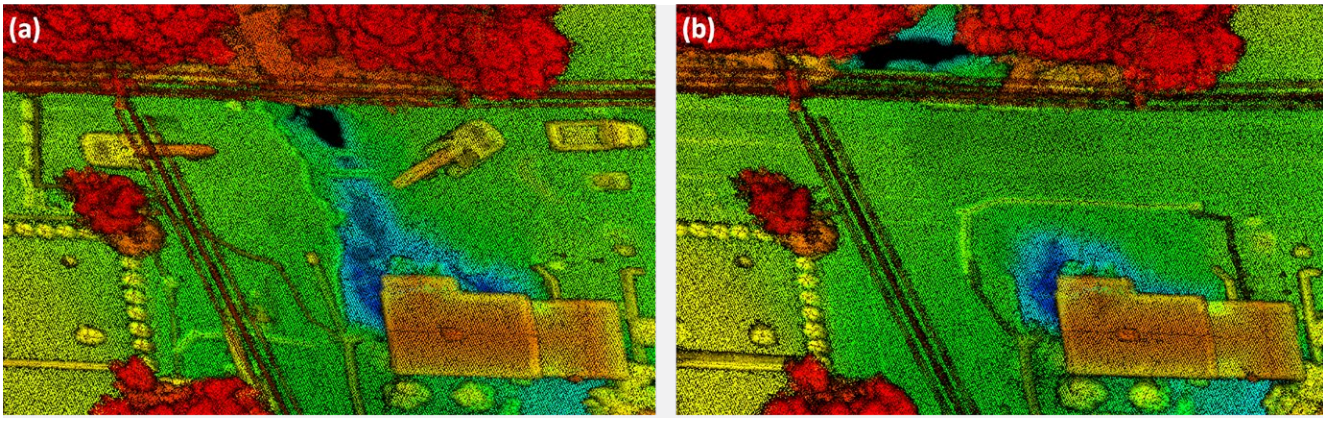

Figure 4: 3DEO's Zion-B sensor captured road washout and repair in Leominster, Massachusetts after a tremendous flood in September 2023. Images are colored blue-to-red according to height, in the range 95–115 m. Imagery obtained on September 14th (a) shows part of the road washed out due to a broken culvert that ran under the road and under a house, exposing underground pipes and the foundation of the house. It also shows barriers on the road, excavators, and support vehicles. Imagery obtained on September 28th (b) shows the repaired section of road that appears darker in intensity due to the lower reflectivity of the freshly asphalted area, and shows the remaining sinkhole around the house. These details and the visible power lines indicate the exquisite detail of target-mode collection type.

the angular diversity is enabled through the geo-referenced scanning capability; and the GM-optimized algorithms process all the views into an aggregated point cloud. 3DEO's second generation system, Zion-B, would have collected the same data quality at a rate exceeding 50 km^2 per hour.

The ability of GM lidar to collect high-density point clouds rapidly at large scale makes it especially suited to disaster response applications. Rapid response timelines are critical for decision makers, so prompt collection and automated processing and exploitation are desirable. An example of rapid deployment and processing is a collection in Leominster, Massachusetts immediately following torrential rain and flooding in September 2023. We performed a dense target collection of 0.26 km^2 size over the worst-hit area. Since the target area is small enough to fit within the field of regard (FOR) of the sensor, for each flight line the entire target is scanned many times from multiple viewing angles, and from 3–4 different flight lines each at different headings. This yields considerable angular diversity and data density, resulting in incredibly detailed lidar products. **Figure 4** shows a section of the target-mode collection around Pleasant Street, performed two days after the flooding and again fourteen days later. Flooding washed out the road, but it had been repaired by the second collection. Possible post-disaster metrics include locating structural

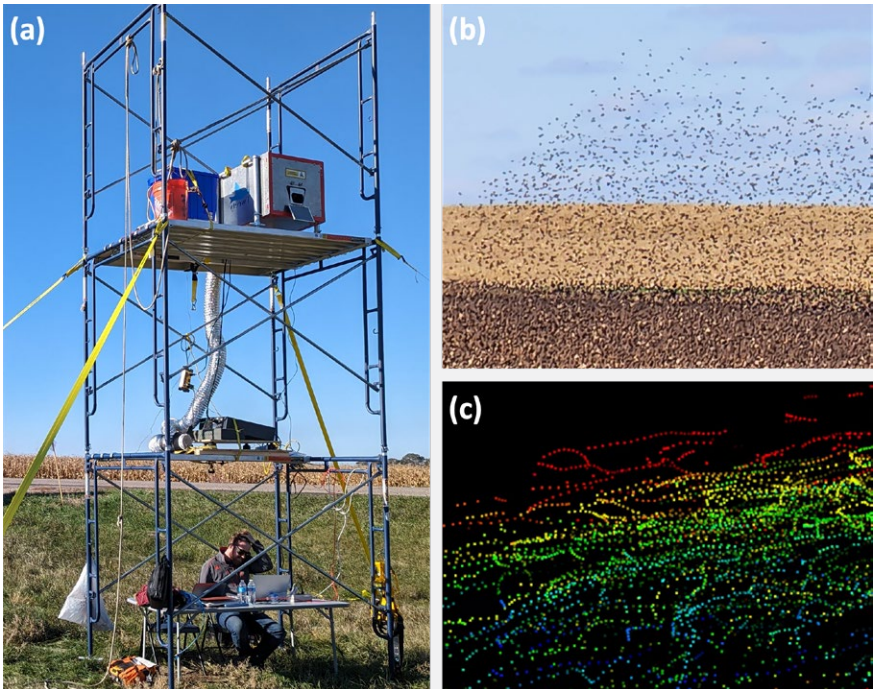

Figure 5: 3DEO's ground-based lidar system, Tweety, developed for real-time bird tracking: (a) sensor setup near Jamestown, North Dakota; (b) flock of red-winged blackbirds being imaged by the lidar; (c) static image of a few seconds of 3D bird tracks where each color represents a unique tracked object and each dot is one step in a multi-second track.

damage, accurate assessment of debris locations and volumes, and powerline continuity. The high resolution of the GM products is anticipated to be a key enabler for accurate decision-support algorithms based on AI/ML.

A natural extension beyond airborne mapping applications is ground-based systems for airspace surveillance. Under SBIR funding from the ARMY ERDC's Geospatial Research Laboratory (GRL), 3DEO developed and conducted proof-of-concept tests of real-time detection and tracking of individual birds within large flocks at standoff distances of approximately 600 m.[7] The high data rates enabled by GM lidars and the use of array-based detectors enable near-video-rate 3D imaging at relevant standoff and field of view for a variety of airspace surveillance applications. **Figure 5** describes one of the field tests.

As GM lidar technology moves from niche and proprietary users into mainstream availability, we hope to see new applications enabled by the high point density, high collection rates, and affordable scalability to wide areas.

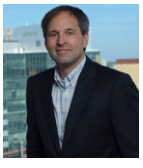

Dale Fried earned his BS in physics from Washington State University and PhD in atomic physics from MIT, studying ultracold trapped atomic hydrogen. After four years at a telecom startup designing integrated optical waveguide structures for wavelength multiplexing, he joined MIT Lincoln Laboratory in 2004, developing and flight-testing airborne GM lidar systems. In 2014 he founded 3DEO, Inc. to commercialize GM lidar technology. Dale is an inventor on 12 patents.

Kimberly Reichel-Vischi has been a lidar scientist at 3DEO since 2019. As an optimist, she is passionate about developing new technologies to improve our world. She earned her BS from the University of Miami and MS/PhD in applied physics from Rice University.

References

1 Khan, M.J. *et al.*, 2024. Remote sensing impact of single-photon sensitive airborne lidar systems based on Geiger-mode avalanche photodiode arrays, *IGARSS 2024 - 2024 IEEE International Geoscience and Remote Sensing Symposium*, Athens, Greece, 2024, pp. 2455-2459; doi: 10.1109/IGARSS53475.2024.10641168.

2 3DEO Scanning: https://www.youtube.com/watch?v=9saTWdozGsc

3 B.R. Call, D. Kelley, D.G. Fried, C. Reichert, K. Reichel-Vischi and A. Eldredge, 2022. Low SWaP, commercially-available Geiger-mode lidar system, *Proc. SPIE 12110, Laser Radar Technology and Applications XXVII*, 1211008, 3 June 2022; https://doi.org/10.1117/12.2619111.

4 B.R. Call, D.G. Fried, D. Kelley and C. Reichert, 2022. Dynamic geo-referenced scanning of aerial lidar systems, *Proc. SPIE 12110, Laser Radar Technology and Applications XXVII*, 121100A,3 June 2022; https://doi.org/10.1117/12.2619105.

5 B.R. Call, D.G. Fried, D. Kelley, K. Reichel-Vischi and C. Reichert, 2024. Assessment of foliage poke-through capabilities of an airborne Geiger-mode lidar, *Proc. SPIE 13049, Laser Radar Technology and Applications XXIX*, 130490I, 5 June 2024; https://doi.org/10.1117/12.3025035.

6 SHR3D: https://github.com/pubgeo/pubgeo

7 A.M. Eldredge, B. Call, D.G. Fried, B. Robinson, T. Mangum, D. Kelley, K. Reichel-Vischi and C. Sturm, 2024. A Geiger-mode lidar system for real-time detection and tracking of individual birds in large dense flocks, *Proc. SPIE 13049, Laser Radar Technology and Applications XXIX*, 1304906, 5 June 2024; https://doi.org/10.1117/12.3025089.

Transform your work with precise **3D scans** and **AR**

RTK
accurate scanning

AR CAD and GIS
overlay

Optimized
GCP workflow

Developed in Switzerland

PIX4Dcatch

Quick, easy, centimeter accurate.

Mobile phone + RTK rover + Pix4D

Compatible with:

EMLID
REACH RX

Trimble
CATALYST DA2

Bad Elf
FLEX
Coming soon

and more

Explore trench scanning and design overlay workflows at
pix4d.com/catch

PIX4D

The U.S. Geodesy Crisis

The current decline in the geodetic capacity in the United States is at a crisis point that is a threat to our economy, international competitiveness and national defense. The current shortage of practicing geodesists, the number of students in the pipeline to become geodesists, and the reduced number of U.S. geodetic academic programs directly undermines the essential role NOAA's National Geodetic Survey (NGS) plays in accurate positioning services nationwide. It more broadly affects any NOAA program that relies on the fundamental geospatial framework, and in particular the programs of the Office of Coast Survey (OCS) and Center for Operational Oceanographic Products and Services (CO-OPS).

In January 2022, the American Association of Geodetic Surveying posted on its website a white paper authored by prominent non-governmental subject matter experts addressing the issue titled "The Geodesy Crisis: America's loss of capacity and international competitiveness in geodesy, the economic and military implications, and some modes of corrective action".

This paper lays bare the need to take immediate action because it takes time to:

- Train geodesists at the remaining geodetic-related academic programs in the U.S.
- Expand the number of geodetic and geomatic programs in the U.S. and populate the programs with students.

Editor's Note: *The following appeared in the September 2023 of the Hydrographic Review Panel newsletter*

What is geodesy and why is it important that the U.S. gains leadership in geodesy-related research and training?

Geodesy is the science of measuring and monitoring the size and shape of the Earth and the location of points on its surface. Without geodesy, the Global Positioning System and other Global Navigation Satellite Systems will not operate properly. Geodesy is the foundation science that supports all navigation, surveying, mapping, timing, geographic information systems, and numerous other activities. This doesn't include the critical role of geodesy to support our troops and the defense of our country.

Geodesy Crisis Impact to the United States

Geodesy underpins most military platforms and systems. If the U.S. geodesy crisis is not resolved, the U.S. government, industry and academia will be unable to compete with Europe, let alone China, in geodesy and geodetic technology. This loss of competitiveness threatens our national security and will cause a dramatic reduction of America's share of the more than $1 trillion per year geospatial economy. The most immediate threat to geodesy in America is the loss of academic training capacity. Without immediate and sustained industrial-scale investment in basic research and graduate training, the few remaining geodesy programs around the country will shrink rather than grow, and America will no longer be able to train itself out of the crisis. The loss of competitiveness would then become permanent.

BY HYDROGRAPHIC SERVICES REVIEW PANEL

THE INVERTED GEOSPATIAL PYRAMID

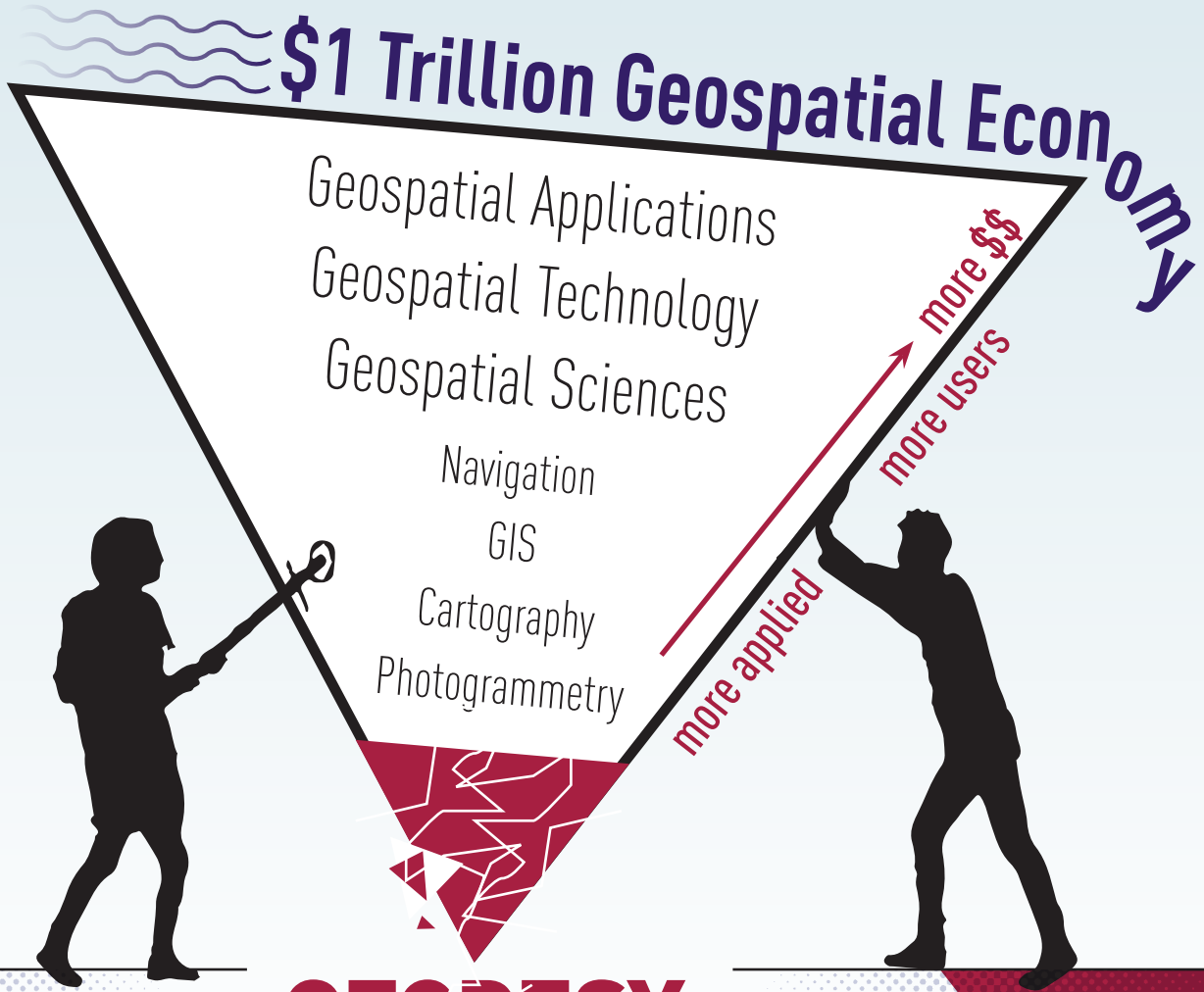

The entire geospatial economy is supported by geodesy!

Current U.S. government agency activities related to the Geodesy Crisis

To address the difficulty filling critical technical geodesy positions with qualified U.S. citizen applicants, leadership from NGS, the National Geospatial Intelligence Agency (NGA), and the National Aeronautics and Space Administration (NASA) have formed the Geodesy Community of Practice. Together these agencies are developing a multi-pronged strategy to increase collaboration and coordination on geodesy education, training, research, fieldwork, and funding opportunities to rebuild the geodesy tradecraft pipeline. Under recent funding levels, NGS' ability to implement many of the recommendations from this group will remain severely limited. In FY 2023, NGS was funded to award ~$4 million in Geospatial Modeling Grants which now provides NGS a direct mechanism to address the crisis, as long as it continues to be funded in the appropriations process into the future.

Why do we have a Geodesy Crisis?

Since the 1990's, U.S. academic programs have reduced focus on geodetic academic research and graduate training in geodesy due to a significant decrease in government funding and associated perceived lack of interest. While the U.S. was reducing geodesy-related research and training, China was dramatically increasing funding and activities in geodesy research and training.

Recommendations for NOAA Action:

- Join the other government leaders and academia in raising the geodesy crisis to the highest level of government to warn of impacts to national security and economic growth.
- Advocate for the designation of geodetic infrastructure as national Critical Infrastructure.
- Support increased investment in the Geospatial Modeling Grants that promote and increase academic and government relationships, training and research activities in geodesy, surveying and related geospatial areas, and rebuild the pipeline for students to follow a geodesy and geomatics career path.
- Sponsor early and mid-career academic training, details, internships, and research work in geodesy and geomatic fields.
- Promote the modernized National Spatial Reference System (NSRS) and communicate the value of an updated, consistent, national coordinate system to support mapping, charting, navigation, infrastructure development, floodplain analysis, resource evaluation surveys, and many other scientific and management applications.
- Endorse requirements for U.S. government agencies to adopt the NSRS for all geospatial data and transition to the modernized NSRS expeditiously upon release.
- Encourage the adoption of the modernized NSRS by state, regional, local and tribal governments as well as the private sector and academia, to make their geospatial data more readily interoperable with government data.
- Proactively engage with national and international geospatial Standards Working Groups, such as the Federal Geospatial Data Committee and International Organization for Standardization to help ensure that the benefits of the modernized NSRS and advances in geodesy are applied to improve socio-economic, environmental, ecological, intelligence, and military programs. ■

In October 2003, Secretary of Commerce Don Evans established the HSRP as directed by the Hydrographic Services Improvement Act of 2002, Public Law 107-372. Panel members, appointed by the NOAA Administrator, include a diverse field of experts.

HSRP MEMBERS 2023

Ms. Mary Paige Abbott
Dr. Nicole Elko
Mr. Eric Peace
Dr. Qassim Abdullah
Mr. Lindsay Gee
Mr. Edward J. Saade
Capt. Anuj Chopra
Ms. Deanne Hargrave
Ms. Julie Thomas (Chair)
Capt. Alex Cruz
Capt. Anne McIntyre
Mr. Gary Thompson
Mr. Sean M. Duffy, Sr. (Vice Chair)
Dr. H. Tuba Özkan-Haller
Mr. Nathan Wardwell

ANYONE CAN TAKE A PICTURE
WE TELL ITS STORY

NV5

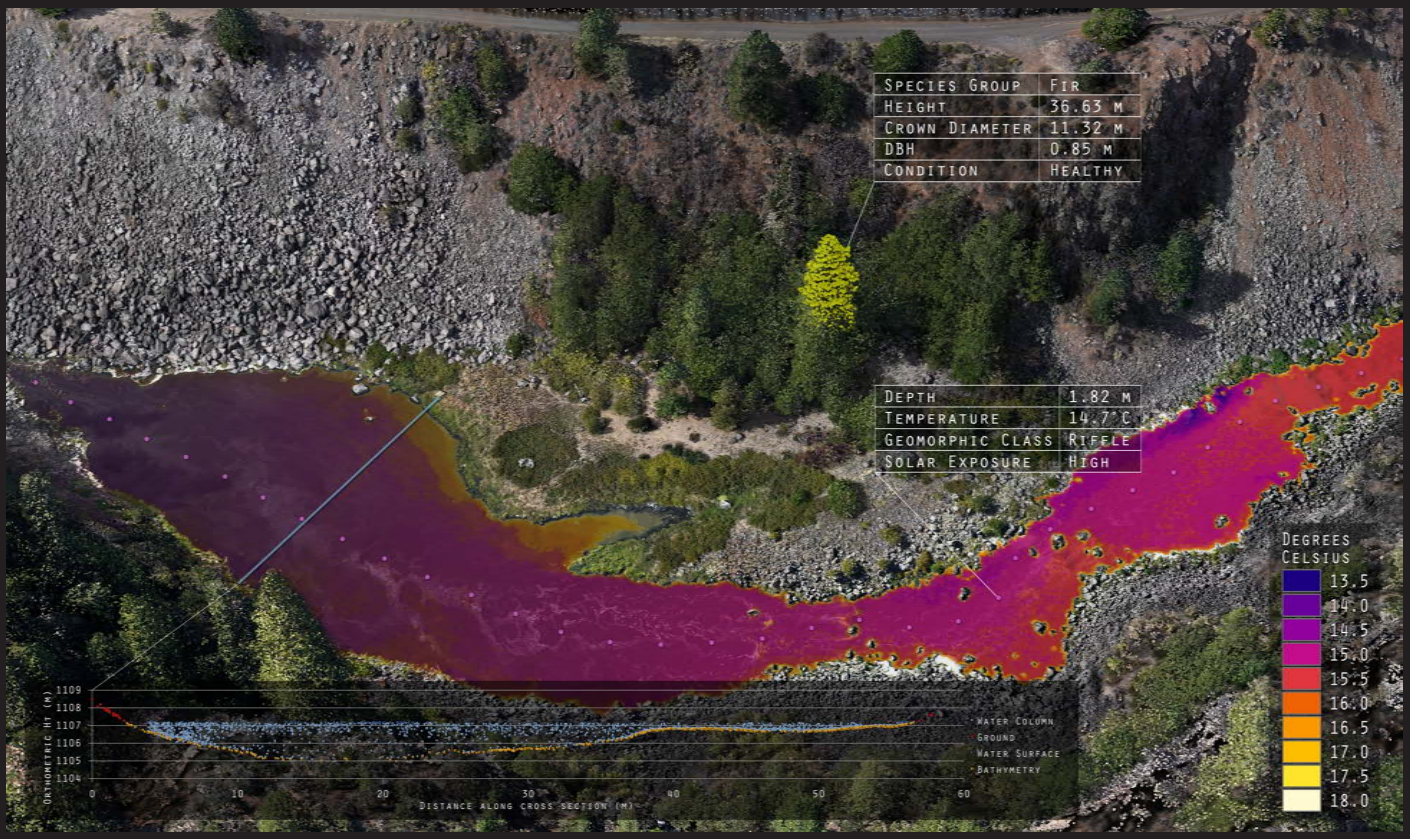

NV5geospatial.com

Sources of uncertainty	Observations	Uncertainties	Values
Navigation uncertainties	$\mathbf{T}^{\mathbf{w}}_{\mathbf{INS}_x}(t)$, Position X of the INS [m]	$\sigma_{\mathbf{T}^{\mathbf{w}}_{\mathbf{INS}_x}}$	Estimated from INS
	$\mathbf{T}^{\mathbf{w}}_{\mathbf{INS}_y}(t)$, Position Y of the INS [m]	$\sigma_{\mathbf{T}^{\mathbf{w}}_{\mathbf{INS}_y}}$	Estimated from INS
	$\mathbf{T}^{\mathbf{w}}_{\mathbf{INS}_z}(t)$, Position Z of the INS [m]	$\sigma_{\mathbf{T}^{\mathbf{w}}_{\mathbf{INS}_z}}$	Estimated from INS
	$\theta_{\mathbf{x}}(t)$, INS Roll [degrees]	$\sigma_{\theta_{\mathbf{x}}}$	Estimated from INS
	$\theta_{\mathbf{y}}(t)$, INS Pitch [degrees]	$\sigma_{\theta_{\mathbf{y}}}$	Estimated from INS
	$\theta_{\mathbf{z}}(t)$, INS Yaw [degrees]	$\sigma_{\theta_{\mathbf{z}}}$	Estimated from INS
Calibration uncertainties	$\mathbf{T}^{\mathbf{INS}}_{\mathbf{LiDAR}_x}$, LiDAR X Lever Arm [m]	$\sigma_{\mathbf{T}^{\mathbf{INS}}_{\mathbf{LiDAR}_x}}$	0.001
	$\mathbf{T}^{\mathbf{INS}}_{\mathbf{LiDAR}_y}$, LiDAR Y Lever Arm [m]	$\sigma_{\mathbf{T}^{\mathbf{INS}}_{\mathbf{LiDAR}_y}}$	0.001
	$\mathbf{T}^{\mathbf{INS}}_{\mathbf{LiDAR}_z}$, LiDAR Z Lever Arm [m]	$\sigma_{\mathbf{T}^{\mathbf{INS}}_{\mathbf{LiDAR}_z}}$	0.001
	Ω, LiDAR Roll [degrees]	σ_{Ω}	0.1
	φ, LiDAR Pitch [degrees]	σ_{φ}	0.1
	κ, LiDAR Yaw [degrees]	σ_{κ}	0.1
Laser scanning uncertainties	$X_0^{\mathbf{LiDAR}}(t)$, mirror center offset in the X direction [m]	$\sigma_{X_0^{\mathbf{LiDAR}}}$	0.001
	$Y_0^{\mathbf{LiDAR}}(t)$, mirror center offset in the Y direction [m]	$\sigma_{Y_0^{\mathbf{LiDAR}}}$	0.001
	$Z_0^{\mathbf{LiDAR}}(t)$, mirror center offset in the Z direction [m]	$\sigma_{Z_0^{\mathbf{LiDAR}}}$	0.001
	$\rho(t)$, LiDAR Distance [m]	σ_{ρ}	0.005 (Given by the constructor)
	$\theta(t)$, LiDAR Horizontal angle [degrees]	σ_{θ}	0.001 (Given by the constructor)
	$\phi(t)$, LiDAR Vertical angle [degrees]	σ_{ϕ}	0.001 (Given by the constructor)

Table 1: 18-parameter total propagated uncertainty for terrestrial lidar systems (Mezian *et al.*, 2016, 334).
Reproduced by permission of the authors.

Nayegandhi, *continued from page 48*
be attributed to systematic errors in the mapping sensor system, i.e., the mapping datum in **Figure 1**. Hence combining these errors provides a statistical estimate of the lidar positional uncertainty for each pulse. For additional information related to topobathymetric lidar, Minsu Kim (USGS) provides an excellent discussion of TPU and absolute accuracy[2].

For airborne topographic lidar, Miloud Mezian and his colleagues divide the uncertainties into three categories[3]:

1. navigational uncertainties: the uncertainty of the absolute position and the platform orientation measured by the inertial navigation system (INS) in real time: factors that can affect the accuracy of the INS include, but are not limited to, errors in measuring pitch, roll, and heading by the inertial measurement unit (IMU), multipath distortion and poor Global Navigation Satellite System (GNSS) geometry
2. calibration uncertainties, including uncertainties in the lever arm and in the boresight angles between the laser scanner and the INS frame
3. laser scanning (and ranging) uncertainties: influences on the laser-target position accuracy, such as weather, surface reflectance, incidence angle on the surface, and the scanner mechanism.

Thus the crux is how to measure and/or verify the three sets (**Table 1**) of input parameters to construct the covariance matrix for the TPU statistics.

Issues surrounding TPU verification

In general, we suggest that the obligation to estimate initial TPU parameters falls primarily on the instrument manufacturers, while verification and testing of the reported TPU value(s) falls on the instrument-user community. Currently, some instrument manufacturers provide estimates for some, if not all, of the instrument (INS, laser, etc.) TPU values. While this is a good start, the user community should be reluctant simply to accept the defaults. In the absence of independent verification, instrument manufacturers could engage in "one-upmanship" and continually tweak the parameter values to make their instruments appear to provide "better" TPUs. The "trust but verify" approach still encourages instrument improvement and innovation while assuring the end-users that the data reports are reliable.

An immediate challenge to arise from the "leave it to the instrument user" approach to verification is the verification methodology itself. Because TPU represents a complex interaction among multiple components and is a statistical estimate, verification precludes a simple test/calibration course or making a physical measurement of one or more components. Minsu Kim suggests that one potential verification method may be to use simulated lidar waveforms to compute TPU[4]. While a lidar waveform simulator could be standardized, even this approach has limitations as each different terrain surveyed would require customized simulation parameters. Additional research may be needed to arrive at a more universal solution.

2 my.asprs.org/ASPRSMember/ASPRS-Member/Events/Event_Display.aspx?EventKey=GW2020PM5

3 Mezian, M., B. Vallet, B. Soheilian and N. Paparoditis, 2016. Uncertainty propagation for terrestrial mobile laser scanner, *The International Archives of the Photogrammetry, Remote Sensing and Spatial Information Sciences*, XLI(B3): 331-335.

4 Kim, M. 2019. Airborne waveform lidar simulator using the radiative transfer of a laser pulse. *Applied Sciences,* 9(12): 2452, June 2019, 16 pp.

Perhaps the final challenge to verifying TPU is the additional cost that will be incurred. Lidar service providers generally work on a fairly tight budget for acquisition and data processing, so any additional data processing will add to the cost of a lidar survey. While the additional cost may be only a small percentage of the survey cost, it may be perceived as superfluous, since there is no huge outcry among lidar end-users for TPU in the first place.

Parting thoughts and recommendations

While simply adding the instrument manufacturer's TPU to the LAS attribute specification is straightforward, making the value meaningful and reliable may be more challenging. To verify the TPU parameters, and hence the TPU value, an independent verification method is required. Simulated waveforms, repeated measurements on the instruments, or some other verification method must be accepted and standardized across the industry. Government and academia should continue to invest in research to derive consistent and standardized TPU and engage sensor manufacturers and data providers from the private sector. End-users may initially resist the additional cost, until the value of TPU is realized in the general community.

We welcome your comments on this topic, and remember, you can also participate and leave comments with the ASPRS Lidar Working Group.

Amar Nayegandhi, CP, CMS, GISP is global head of technology and innovation at Woolpert. He is responsible for aligning, optimizing, integrating, and expanding Woolpert's technology portfolio across its globally integrated architecture, engineering, and geospatial platform. Amar is an ASPRS Fellow and was the director of the ASPRS Lidar Division. He co-edited the ASPRS DEM Users Manual, 3rd Edition and authored the chapters on airborne topographic lidar and airborne lidar bathymetry. Before joining Woolpert, Amar served as senior vice president at Dewberry, where he led the firm's geospatial and technology services operating unit. Prior to that, he managed federal coastal science and resource management contracts at Jacobs, where he developed algorithms and post-flight data processing software for government-owned topographic and bathymetric airborne lidar sensors used in research.

Al Karlin, Senior Geospatial Scientist, Dewberry, serves as a consultant on Florida-related lidar, topography, hydrology, and imagery projects.

The case for (and against) propagated uncertainty in aerial topographic lidar, continued!

Total Propagated Uncertainty must take into account the relationships between the datums defined by the ground control points and the inertial navigation system, as well as the characteristics of the lidar sensor and the circumstances of its use. Adopting the default TPU given by the sensor manufacturer is insufficient.

We ended the previous *Full Coverage* column with parting recommendations on incorporating some form of Total Propagated Uncertainty (TPU) into the LAS format, focusing on airborne lidar data. We noted that for TPU to be truly useful we must safeguard the integrity of the information with independently verifiable methods, which could attract additional costs. This time, we would like to pick up that thread and elaborate on how to accomplish a meaningful TPU.

Measuring mapping surfaces

In the spring 2024 issue of ***LIDAR Magazine,*** our colleague, Qassim Abdullah, eloquently addresses the issue of true, survey (pseudo) and mapping datums[1]. **Figure 1** illustrates how these three datums are related. There is the true surface (i.e. the earth), a survey/control point pseudo-surface, and the surface mapped by the lidar sensor.

For most topographic lidar surveys, we take the survey surface as "ground truth" and adjust the mapping surface accordingly, even though there is propagated error in the survey surface that may not be properly integrated into the final solution, as per Qassim's commentary.

This whole process of adjusting the mapping surface to the survey (pseudo) surface works acceptably well provided that the survey surface is more accurate (see Qassim's commentary on accuracy) than the mapping surface and is properly processed. But what happens when we cannot measure a survey surface, as in the case of acoustic bathymetry or topobathymetric lidar? Moreover, we cannot possibly measure the survey surface at every location where we have a lidar data point. That's where TPU can provide an additional metric to determine how close the mapping datum is to the true surface.

1 Abdullah, Q., 2024. Best practices in evaluating geospatial mapping accuracy according to the new ASPRS accuracy standards, *LIDAR Magazine*, 14(2): 37-46, spring 2024.

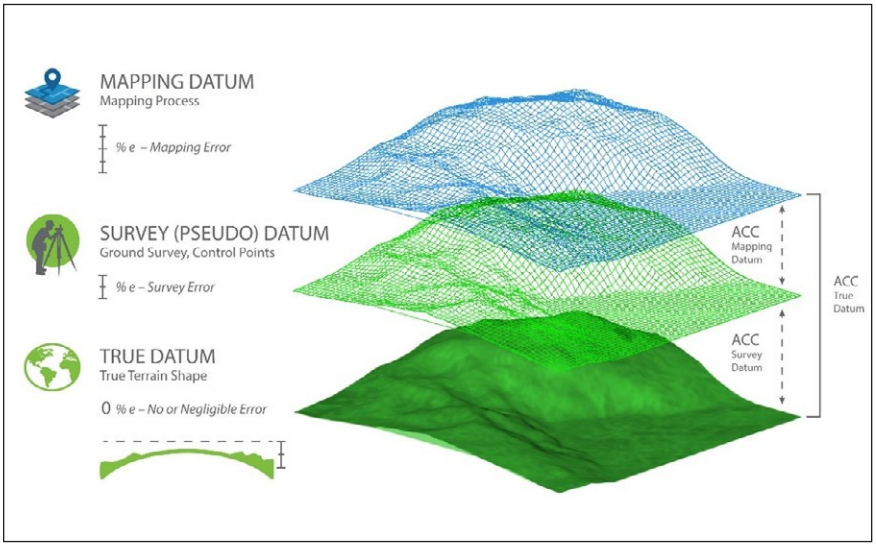

Figure 1: Datums and error propagation in geospatial data (Abdullah, *ibid.*, 40).
Reproduced by permission of the author.

TPU without the survey (pseudo) datum

The recent history of TPU for bathymetric lidar and, now, by extension, topographic lidar, begins in 2013 with an 11-parameter TPU model presented at the Joint Airborne Lidar Bathymetry Technical Center of Expertise (JALBTCX) workshop in 2013. This has undergone several revisions, resulting in the current 17-parameter TPU model. It is beyond the scope of this column to describe these models—suffice it to say that they attempt to describe the horizontal and vertical errors that can

continued on page 48

LiDAR USA

3D MAPPING SOLUTIONS

Surveyor 120 UAV LiDAR System

$29,990.99 ONLY

Includes: Rev120 UAV LiDAR System, Subscription Software, Basic Mount, and Battery
Not Included: Training, Drone, Cameras, MMS and Shipping

STONEX
U.S.A.

XVS

VISUAL SLAM

vSLAM 3D Scanner

COME SEE US
GEO WEEK

Stonex USA | 54 Regional Dr. | Concord 03301 - New Hampshire
For a Stonex dealer near you contact us:
Phone: 603-715-5771 | sales@stonexamerica.com
www.stonexamerica.com